Student Declaration of Authorship

HERIOT WATT UNIVERSITY
UK | DUBAI | MALAYSIA

Course code and name:	F21MP Masters Project and Dissertation
Type of assessment:	**Individual**
Coursework Title:	F21MP Masters Dissertation
Student Name:	Elliot Whitehouse
Student ID Number:	H00359236

Declaration of authorship. By signing this form:

- **I declare** that the work I have submitted for individual assessment OR the work I have contributed to a group assessment, is entirely my own. I have NOT taken the ideas, writings or inventions of another person and used these as if they were my own. My submission or my contribution to a group submission is expressed in my own words. Any uses made within this work of the ideas, writings or inventions of others, or of any existing sources of information (books, journals, websites, etc.) are properly acknowledged and listed in the references and/or acknowledgements section.

- I confirm that I have read, understood and followed the University's Regulations on plagiarism as published on the University's website, and that I am aware of the penalties that I will face should I not adhere to the University Regulations.

- I confirm that I have read, understood and avoided the different types of plagiarism explained in the University guidance on Academic Integrity and Plagiarism

Student Signature *(type your name):* *Elliot Whitehouse*

Date: *15/08/2022*

Copy this page and insert it into your coursework file in front of your title page.
For group assessment each group member must sign a separate form and all forms must be included with the group submission.

Your work will not be marked if a signed copy of this form is not included with your submission.

Optimisation of Microgrid Design Considering the Presence of Electric Vehicles

Elliot Whitehouse

15 August 2022

Declaration of Authorship

I, Elliot Whitehouse, declare that this thesis titled, 'Optimisation of Microgrid Design Considering the Presence of Electric Vehicles' and the work presented in it is my own. I confirm that this work submitted for assessment is my own and is expressed in my own words. Any uses made within it of the works of other authors in any form (e.g., ideas, equations, figures, text, tables, programs) are properly acknowledged at any point of their use. A list of the references employed is included.

Signed: Elliot Whitehouse

Date: 15 August 2022

Acknowledgments

I would like to thank Dr. Lilia Georgieva and Dr. Hani Ragab for their guidance and support during the planning of this research project. Their knowledge and expertise have been invaluable.

Abstract

As the climate crisis worsens and global demand for electricity rises, more renewable energy sources (RES) must be integrated into power networks. However, the distributed nature of many RES make it a challenge to integrate them into traditional grid power networks characterised by centralised generation and control. This has led to the development of the microgrid (MG) concept; low voltage distribution networks that are composed of a variety of distributed energy resources (DER) (often renewable in nature) placed close to local loads with a control and management system underpinned by a communications infrastructure. The environmental and economic benefits of MGs make them an attractive alternative to the traditional centralised network.

Designing an MG is a complex task requiring the consideration of many variables. Once of which that is becoming increasingly prevalent is the management of electric vehicles (EV). Left uncontrolled, the charging of EVs can cause significant disruption to MGs and the benefits of their presence never realised. Through the vehicle-to-grid (V2G) concept, EVs can be used to store excess energy, reduce peaks in demand and provide voltage and frequency regulation services to the MG. The design of MGs and strategic charging of EVs is an optimisation problem, to which metaheuristic algorithms are particularly suited. The aim of this project is to optimise the design of an MG and EV charging strategy using a multi-objective genetic algorithm (GA) to minimise costs and emissions of the MG.

Contents

List of Figures

List of Tables

Chapter 1

Introduction

Global demand for electricity rose by more than 6% during 2021, higher than any year following the recovery from the financial crisis in 2010 (IEA 2022). This led to global carbon dioxide (CO2) emissions from electricity generation hitting an all-time high as more coal and gas was used to meet this rapidly increasing demand despite the growth in renewable power (IEA 2022).

The COVID-19 pandemic also impacted the electricity market. Debnath et al. 2021 found that lockdown in the UK lead to substantial shifts in household patterns of electricity consumption that have continued even after lockdown. This, alongside the increasing pervasiveness of digital connected devices and Electric Vehicles (EVs) in residential settings, is leading to a larger and more unpredictable household demand for electricity.

As demand for electricity is increasing, so are the negative effects on

the environment. It is widely known that one of the most important ways to combat this and reduce CO2 emissions is through the use of Renewable Energy Sources (RES) for the generation of electricity.

Many types of RES, including photovoltaics (PV), small wind turbines (WT) and combined heat and power (CHP) systems, are a type of Distributed Generation (DG) which falls under the banner of Distributed Energy Resources (DER). DERs, in contrast to the conventional centralised system, are energy technologies, including DGs and Energy Storage Systems (ESS), placed near to consumers and are connected to energy distribution networks (Mehigan et al. (2018), Ren & Gao (2010)).

Distributed energy systems offer several benefits over the centralised system: locating DG near end-users minimises transmission and distribution losses, allows for increased flexibility and control over the local distribution network and have sustainability benefits through the integration of RES (Alanne & Saari 2006). Therefore, distributed energy systems are increasingly seen as the future of energy systems (Zahedi (2011), Anestis & Georgios (2019)).

Despite the benefits of distributed energy systems, the integration of DERs on a large scale presents significant technical problems for distribution networks that will require state-of-the-art monitoring and control strategies to mitigate; this has led to the development of the microgrid (MG) concept (Lopes et al. 2013).

MGs are Low-Voltage (LV) distribution networks that are composed of a variety of DERs placed close to local loads and a control and management sys-

tem underpinned by a communications infrastructure (Quiggin et al. (2012), Ramachandran et al. (2013), Patrao et al. (2015)). MGs have two modes of operation, grid-connected mode where power is exchanged with the upstream High-Voltage (HV) and Medium-Voltage (MV) distribution network, or they can be operated in island mode where they are isolated from the upstream distribution network and the DERs present in the MG supply energy to consumers (Katiraei & Iravani 2006).

MGs have several benefits over the traditional centralised distribution network which has sparked much research and investment over the last decade (Lotfi & Khodaei 2017). The DERs in MGs are mostly RES (Fathima & Palanisamy 2015) such as WT and PV which reduce Geenhouse Gas (GHG) emissions in the production of electricity. In addition to their environmental benefits, MGs reduce power losses and provide support to regulate voltage and frequency (Zia, Elbouchikhi and Benbouzid 2018 (Zia et al. 2018)).

A key challenge for MGs with a high penetration of RES is their reliance on suitable weather conditions. Weather conditions can be highly variable and unpredictable, leading to the output of RES being intermittent and stochastic in nature. This is a problem for end-users who are used to being able to consume as much power as they like whenever they like, where production increases to meet demand. The installation of ESS alongside RES in the MG can mitigate these effects (Quiggin et al. (2012), Fathima & Palanisamy (2015)). When weather conditions are favourable and output from RES is high and demand is low, the ESS can be charged. In times of high demand but low output, the ESS can be discharged to fill the gap in supply. However, despite ESS facilitating the integration of RES in MGs,

progressively increasing demand will put a strain on MGs with a high degree of RES penetration.

A global focus on reducing CO2 emissions has driven the growth of the EV market considerably and the COVID-19 pandemic did little to slow this down. EVs share of global car sales more than tripled between 2019 and 2021 rising from 2.5% to close to 9% (Paoli & Gül 2022). This trend is reflected in the UK which has seen a 23.161% increase in licensed plug-in electric vehicles (PEVs), which constituted 1.49% of the total number of licensed cars (excluding all other vehicle types) (DfT 2022). This is set to increase with roll-out of government initiatives such as the Office for Zero Emission Vehicles (OZEV) plug-in car grant (UK 2022), and the UK government's commitment to end the sale of all new petrol and diesel cars and vans by 2030.

While the uptake in EVs is helping to reduce CO2 emissions in the transport sector, it is having a significant impact on the electricity market. A single EV can cause a 50% increase in the electricity consumption of a single household (Brouwer et al. 2013) and with EVs projected to account for 60% of new car sales by 2030 (IEA 2021), this will cause a significant problem for the grid, particularly if charging is uncontrolled (Hadley & Tsvetkova 2009).

On the other hand, a high penetration of EVs can benefit an MG. Through the vehicle-to-grid (V2G) concept introduced by Kempton & Letendre (1997) whereby EVs can feed power back to the grid, they have the potential to be used as independent DERs that can balance the intermittency of RES, and provide ancillary services such as peak power shaving, spinning reserve,

voltage and frequency regulation (Mwasilu et al. 2014).

1.1 Aims and Objectives

This project aims to optimise the design of a residential microgrid with different penetration levels of EVs whereby the electric vehicle batteries are used to provide peak load shaving and V2G services to the microgrid.

1.1.1 Objectives

1. Use Multi-Object Optimisation to optimise the mix and sizing of distributed energy resources to minimise the costs and environmental impact of the MG considering different penetration levels of EVs.

2. To minimise the environmental impact of the designed MG using EV batteries to provide services to the grid using centrally controlled charging and discharging strategies.

3. To maximise the level of autonomy of the designed MG from the upstream grid using EV batteries to provide services to the grid using centrally controlled charging and discharging strategies.

1.1.2 Secondary Objectives

1. To model the usage of home appliances and include their scheduling in the optimisation of the MG.

2. To optimise the topology of the MG considering power losses and efficiency.

1.2 Manuscript Structure

Firstly, in section 2, a background will be given about MGs, explaining their structure and design considerations. Then a review of the related literature in MG optimal design will be given in section 2.2.1, detailing the types of optimisations used to solve the MG planning problem. Following this in section 2.3, a background of EV charging control strategies is given followed by a review of the related work, categorised by control type.

Then, the modelling and simulation will be explained, starting with the load and component modelling in section 3.2, followed by a presentation of Multi-Agent System (MAS) being used to simulate a MG in section 3.3. In this section, details of the model, geospatial component and agents is given in addition to the rules of their interaction. Following this in section 3.4 the optimisation algorithm is presented , explaining the objectives, design space, implementation and a description of the testing scenarios.

Section 4 contains the results and discussion followed by a review of whether this paper has met the objectives set out in section 1.1.1

Chapter 2

Background and Literature Review

In this section an overview of MG is given, describing their types, features and design considerations. Then, MG design optimisation methods are introduced followed by a discussion and critical evaluation of related research. Subsequently, an overview of EVs and their impact on MGs is provided. This is supplemented by a critical review of previous work into the scheduling of EV charging in MGs and how EV batteries can be utilised to provide services to MGs.

2.1 Microgrids

There are 3 main categories of MG: Alternating Current (AC), Direct Current (DC) and hybrid AC/DC systems. AC MGs have one or more AC buses and

any loads or DGs that are not AC in nature must be connected via a power electronic interface such as a DC/AC converter (Das & Balakrishnan (2012), Basak et al. (2012)). DC MGs consist of DC buses connected to DC DGs and loads and are connected to the upstream grid through an AC/DC converter. In DC MGs, AC power sources such as wind turbines and diesel generators are integrated using AC/DC converters (Roslan et al. 2019). The AC/DC hybrid system consists of an AC MG with a DC sub-grid connected through an AC/DC converter (Loh et al. 2013).

AC MGs are the easiest to integrate into the main upstream AC grid, however many complex power electronic interfaces are required to integrate DC DERs into the system, reducing its efficiency and reliability (Deng et al. 2013). DC MGs avoid this issue, however, the use of a power electronic converter to connect the MG to the upstream grid can negatively impact reliability and efficiency in the exchange of power with the upstream grid (Planas et al. 2013). On the other hand, hybrid MGs combine the advantages of AC and DC MGs by having a direct connection to the upstream grid and reducing the need for complex power electronic converters (Patrao et al. 2015). These benefits make hybrid AC/DC MGs and attractive option for future power system design (Lotfi & Khodaei 2017) and so will be the baseline system used in this paper.

2.1.1 Microgrid Planning

The planning of each MG has unique considerations, however Gamarra & Guerrero (2015) identify three common problems in the planning of all MGs:

- Determining the optimal selection and sizing of DGs and ESS considering cos-effectiveness, environmental impact, reliability and quality goals.
- The location of DERs and layout of power lines considering power loss and quality
- The scheduling of DERs to achieve systems goals determined by demand, operational and system constraints and transmission capabilities.

While there exists multiple objectives in the optimisation of MG planning, in most studies focussing on one objective, it is economic in nature (Wasilewski (2018), Nikmehr & Ravadanegh (2015)). However, an important consideration in the reduction of GHG emissions from the production of electricity is the MGs level of autonomy from the grid. The greater the proportion of energy supplied by RES within the MG, the lower its environmental impact will be.

2.2 Microgrid Planning Optimisation

MG planning is an optimisation problem, and, in the literature, various optimisation techniques have been utilised to solve it. Predominantly optimisation techniques chosen by researchers fall into one of two categories: metaheuristic techniques and non-metaheuristic techniques. In the following section, related works in both of these fields are reviewed and critically evaluated.

2.2.1 Related Work

2.2.1.1 Non-Metaheuristic Techniques

Omu et al. (2013) introduce a distributed energy network optimisation model that utilises MILP to optimise the selection, size, and location of DERs in addition to the distribution network structure, with the aim of minimising annual investment and operating costs. The model is solved using the CPLEX solver provided by the IBM ILOG CPLEX Optimisation Studio. The cost objective function to be minimised consisted of investment, operation and maintenance, electricity and fuel costs minus the revenue generated from selling energy to the upstream grid or from energy subsidies. The model was tested using a case study of a neighbourhood in the UK with one day representing each season split into 24 - 1 hour time periods. Average weather data for each season was used to calculate the output of PV and wind systems.

Results were compared with a base case of energy being supplied by the main UK grid and it was found that while optimally designed DER systems have higher investment costs, the provide a higher Net Present Value (NPV) over time than the base case and can reduce annual CO2 emissions. However, emissions are only considered as a constraint in the model and not as a design parameter.

Wang et al. (2014) propose an MG planning methodology formulated as a Mixed-Integer Program (MIP) to optimise the location, size and types of DGs with the objectives of minimising total costs and maximising profits. The total costs include investment, operation and maintenance, fuel and

emission costs while the profits include the revenue generated from selling electricity to consumers within the MG and the upstream grid. Case studies use WT, PV and MT and DGs. The model is transformed into a two-stage robust optimisation problem, solved using a column and constrains generation framework where uncertainty in the output of RES is considered using polyhedral uncertainty sets. The model is then tested on an IEEE 33-bus distributions system over a planning horizon of 20 years.

Results showed that while the locations of DGs remained consistent in different instances where different initial budgets were used, the sizes of the DGs differed. The researchers compared their model to a deterministic one proposed previously and found that profits were larger when using the deterministic model. The researchers conclude this is because their model accounts for uncertainty in load demand and DG output and therefore is more conservative in its calculation of profits.

The strengths of the researcher's approach are making uncertainty in load demand and DG output a central part of their methodology and including emissions costs in their calculation of total costs.

However, the researchers in the previous two papers do not consider the use of ESS to complement the intermittency of RES and supplement supply in times of high demand.

Chen et al. (2012) presented a mixed-integer linear program (MILP) for optimal sizing of ESS in an MG based on a cost-benefit analysis. The algorithm was implemented in A Modelling Language for Mathematical Programming (AMPL) with CPLEX. Time series techniques were used to fore-

cast wind speed based on historical data from the past year in Singapore, and Feed-Forward Neural Networks (FNN) were used for forecasting the solar radiation based on the previous months weather data. The solution was tested on two case studies, one where the MG was operated in grid-connected mode and the other where the grid was operated in island mode. For the grid-connected case study, the objective was to maximise the total benefit which comprised of the revenue generated from selling energy to the upstream grid, minus the cost of electricity generation (from Fuel Cell (FC), Microturbine (MT), PV and WT). Whereas in the islanded mode case study, the objective was to minimise the total costs, made up of the investment, installation and maintenance costs of the ESS plus the cost total cost of electricity generation.

It was found that increasing the size of ESS in the MG increased the benefit in grid-connected mode by 2% per day compared to an MG with no ESS and decreased the cost in islanded mode by 8.64% per day compared to an MG with no ESS. It was also found that having optimally sized ESS in the MG reduced the total cost by smoothing out the power supply and therefore reducing the start-up and shut down costs of generators; can help to regulate grid frequency; and act effectively as a reserve capacity when load demand is high and generation is low.

However, the time horizon for the case studies is only one day and so does not account for seasonal variation in load demand or weather which impacts the generating capacity of the PV and WT. In addition, while the consideration of forecasting errors for wind speed and solar radiation using Root Mean Square Error (RMSE) and Mean Absolute Percentage Error (MAPE) respectively accounts for some of the uncertainty inherent in RES, it does

not go far enough in capturing the stochastic nature of RES and the uncertainty of energy generated by RES. The researchers also do not consider the capacity of the other DERs in the MG or emissions.

In the non-metaheuristic approaches reviewed in this section, the researchers focus on one objective: the cost of the MG. While costs are a crucial element of the planning process, they either ignore or do not capture the complexity of a multitude of other factors present in MG planning decisions such as GHG emissions or the level of MG autonomy from the upstream grid.

When multiple objectives are present, they may often conflict with each other. For example, while increasing the number of RES and ESS decreases the environmental impact of the grid and increases its energy autonomy, it will also increase the cost (Omu, Choudhary and Boies 2012). Therefore, minimising MG cost and maximising energy autonomy are mutually exclusive. In this scenario, optimisation techniques are required that can find a balance between the conflicting objectives that will provide an optimal solution. Metaheuristic algorithms can deal effectively with multi-objective problems making them well suited to the MG planning problem and this approach has been popular in this area of research (Katsigiannis, Georgilakis and Karapidakis 2010).

2.2.1.2 Metaheuristic Techniques

Kefayat et al. (2015) used a hybrid of Ant Colony Optimisation (ACO) and Artificial Bee Colony (ABC) algorithms to optimise the placements and size

of DERs in a distribution system. A multi-objective ABC is also used to produce a set of non-dominated solutions of the algorithm with the objectives of minimising power losses, total emissions, total electrical energy cost and improving voltage stability. They considered gas turbines, fuel cells and wind turbines as DERs and modelled the uncertainty of wind and load using Weibull and normal distribution functions respectively. The algorithm was tested on the IEEE 33- and 69-bus test distribution systems using MATLAB, however it was found that the algorithm underperformed from a technical, environmental and economic point of view when compared to other evolutionary approached such as PSO CFA, ABC and Modified Teaching-Learning Based Optimisation (MTLBO).

Particle Swarm Optimisation

Samadi Gazijahani & Salehi (2017) propose a stochastic multi-objective optimisation framework to optimise planning of interconnected MGs considering economic, technical, reliability and environmental uncertainty. Using Multi-Objective Particle Swarm Optimisation (MOPSO), the site, size, type and time of investment of DERs in MGs is optimised along with the allocation of section switches to partition a conventional distribution system into interconnected MGs. The approach is tested on an 89-bus distribution network over a planning horizon of 10 years where the costs and reliability are calculated for each year. DERs considered are wind turbine (WT), photovoltaic (PV) and combined heat and power (CHP), where the stochastic nature of wind and solar power are modelled using the Weibull and Beta probability density function (PDF) respectively. Loads are also seen as stochastic and

so are modelled using the normal distribution function. Using these PDFs, Monte Carlo simulation is used to generate 1000 scenarios of wind speed, solar radiation and load which is then reduced to 30 using a backwards scenario reduction technique. For the Energy Storage System (ESS), it is assumed that it is fully charged during times of low load during the day and discharged in the day's peak load hour.

The objective functions considered are the total economic costs and reliability costs. Economic costs include investment costs, maintenance costs, fuel costs, pollution emission cost and power losses cost whereas reliability costs include the cost of grid connected mode energy not supplied and islanded mode emery not supplied. Once the MOPSO optimisation has been run, the membership function of each objective function is calculated to determine the optimal solution for each of three risk profiles: risk-seeking, risk-neutral and risk averse. These are then compared in terms of their cost and reliability. The three risk-aligned optimal solutions are compared to a tradition method for solving the MG planning problem. It is found that the proposed approach outperforms the traditional approach in terms of voltage profile, power losses and energy not supplied (ENS).

The stochastic nature of loads and RES are well considered in this paper and the approach outperforms traditional methods; however, the costs and reliability are only considered on a yearly basis, considering the peak load for that investment year. The intricacies of how load demand fluctuates seasonally throughout the year are not considered at this level of observation. In addition, only a static model is considered for the ESS which assumes there will be enough available energy to fully charge the ESS each day so it can be

discharged in the peak hour. This does not consider the dynamic relationship between DGs and ESS at varying times of the day. Finally, the researchers only evaluate the solutions from an economic perspective.

Genetic Algorithm

Katsigiannis et al. (2010) investigated the use of the NSGA-II algorithm to optimise the size of components in small autonomous hybrid power systems to improve economic and environmental performance. The objective functions in the study were: the cost of energy, accounting for annualised capital costs, the annualised replacement costs, the annual operation, and maintenance (O&M) costs, the annual fuel costs, and the discount rate utilised; and GHG emissions based on life cycle analysis (LCA) that considers the GHG throughout the entire life of a component from the extraction of raw materials to shut down and disposal. They compared the performance of systems with lead-acid batteries as ESS and hydrogen storage. It was found that systems that used lead-acid batteries performed significantly higher from both an economic and environmental perspective compared to hydrogen storage. The researchers also found that the Pareto optimal solutions for both lead-acid and hydrogen ESS systems favoured a high number of WT and ESS over PVs due to the high economic cost of the latter. Whereas in the hydrogen system, there is a significant increase in the size of FC due to the use of hydrogen fuel compared to the lead-acid battery system which uses natural gas as fuel. This is due to the high economic and environment cost of FC using natural gas as fuel.

Zidan et al. (2015) used a multi-object GA to optimise the capacity sizes and types of DG for a combined heat and power system within MGs. The two objectives were to minimise total net present cost and carbon dioxide emissions. The DGs considered are natural gas fuel cells (NGFCs), hydrogen gas fuel cells (H2FCs), natural gas turbines) (NGTs), thermal storage T(S), WT, and PV. The uncertainty of wind speed and solar irradiance are modelled using the Weibull and Beta distributions respectively. A year is divided into three seasons (winter, mid-season and summer) and each season is represented by one sample day which is split into time steps of 24 hours. For each hour, the PDFs of the wind speed and solar irradiance are split into 12 and 10 states respectively, the probabilities of which are convolved giving 120 states for each hour.

The study found that NGT perform better than FCs in reducing net present cost and H2FC outperform NGT and NGFCs in reducing GHG emissions. Modelling the uncertainty of wind speed and solar irradiation using PDFs in this study captures the stochastic nature of the output from WTs and PVs compared to using historical data alone. However, this study does not consider the placement of DGs within the MG, power loss or MG autonomy level and simulations are only run over 3 days which are representative of 3 seasons within the year. This time horizon for simulation is not long enough and does not capture the nuance of energy demand and production changes throughout the year.

Sachs & Sawodny (2016) formulate a three stage multi-objective design optimisation for island microgrids to minimise economic and environmental objectives. Capital expenditure (investment costs), LCOE and emissions are

the objective functions to be minimised. In the first stage, they determine representative load profiles using k-Means clustering. The second stage determines the optimal sizing of the system components and power electronics layout. Finally, the third stage determines the optimal power dispatch strategy. They use detailed modelling of PV, BESS and diesel generator systems, accounting for diesel generator cold start/shutdown cost, start-up/shut down times, a penalty for operating under minimum load and appropriate BESS properties. NSGA-II and Non-Linear Mesh Adaptive Direct Search method (NOMAD) are applied to solve the optimisation problem and their results compared.

The simulation was run with 10 min time steps over time horizons ranging from 1 day to 1 year. PV power and load demand data are taken from a Philippine village while the weather profile is taken from New Delhi. Similar solutions were found by the NOMAD and NSGA-II algorithms, however, in the case of NOMAD, some solutions lay off the Pareto front due to the algorithm becoming stuck in local optima. The performance of the algorithm was compared to that of the commercially available software tool for optimising MG design, HOMER. It was found the proposed multi-objective three stage approach resulted in a 10% reduction in LCOE and a 70% reduction in computation time compared to the system design by HOMER.

While the detailed system modelling in this study captures a realistic level of detail, the mixture of data to simulate the MG is not representative of a real-world situation. The researchers also do not consider the location of DGs and their impact on power quality in the MG. The impact of EVs is also not included.

Moghateli et al. (2020) propose 2 multi-objective approaches for the optimal design of multiple MGs in an Active Distribution Network, where the sites of sizing of ESS and the locations of sections switches are the decision variables. The multi-objective optimisation problem is solved using NSGA-II. In approach 1, the objectives are to improve reliability and self-adequacy (each MGs ability to be self-sufficient in the multi-MG distribution network) in addition to minimising the annual cost of losses and power from the upstream distribution network. Approach 2 includes the same objectives functions of approach 1 with the addition of a new probabilistic index for the ratio of storage to load capacity in each MG. The minimisation of the load-storage ratio decreases the impact of load uncertainty on the MG as the lower the ratio, the more closely aligned the total ESS storage capacity is to the load demand and therefore energy received from the upstream grid is minimised.

The researchers use WT and PV as DGs in the MG and model the uncertainty of their generation using Weibull and Beta PDFs respectively as in Samadi Gazijahani & Salehi (2017). The uncertainty of load is also considered by using a normal PDF where the mean and standard deviation are taken from historical data. As opposed to, Samadi Gazijahani & Salehi (2017), in this study ESS are modelled so that they are charged/discharged based on DG generation and load demand, accounting for the dynamic relationship between production and demand. The model is simulated over one year, taking an average day of each month as representative of each month of the year, giving 12 simulation days. Due to the probabilistic model of generation and load, Monte Carlo simulations are run for each hour of each day to produce the data used in calculations of the objective functions. The al-

gorithm is tested on a 33- and 119-bus distribution network. The researchers found that approach 2, with the inclusion of the load-storage ratio, outperformed approach 1 in terms of cost, reliability and load uncertainty, despite a decrease in self-adequacy.

Despite the modelling of the ESS that captures more detail of the role of ESS in an MG, the researchers fix the number and rated capacity of the ESSs, limiting the search space of the algorithm leaving the possibility of potentially more optimal solutions. The optimality of DG location is not considered as DG locations are predetermined. The impact of EVs is also not considered.

Dougier et al. (2021) developed a decision support tool to design various microgrids that provide compromises for MG designers in terms of economic, technical and environmental objectives. The three objectives present in this study are minimising the levelized cost of energy (LCOE: the total cost over the lifetime of a power plant divided by its produced energy), greenhouse gas emissions (GHG) and maximising the MGs autonomy from the upstream grid. The NSGA-II algorithm was used to optimise the design parameters of the MG including the size of DGs (WT, PV, gas and biomass power plants, BESS and pumped-hydroelectricity energy storage (PHES)) and the management strategy of the MG. The management parameters able to be set by the decisions maker are the MG control strategy which defines the relationship between production, demand and storage, and the priority order in which DGs are solicited to meet demand and supply energy for storage.

The MGs are evaluated using a sequential simulation in MATLAB using

meteorological and load demand data as inputs. The time horizon of the simulation is one year, whereby data for the average weekday each month is taken as representative of that month in order to account for seasonal fluctuations in production and demand. Each of the 12 simulation days is then broken down into 90-minute time steps and the production and consumption is calculated for each time step. Input data for solar radiation, wind-speed and load are taken from Aix-en-Provence, assuming 7000 homes in the proposed MG.

The researchers perform two multi-objective optimisations considering LCOE and GHG in the first and LCOE and autonomy level in the second. They found the solutions presented along the Pareto-front in each optimisation was an effective way to provide MG decision makers with a variety of MG designs that consider economic, technical and environmental objectives.

The inclusion of the MG management strategy as decision variables is a novel approach compared to other research and considers the objectives of the MG decision maker whereas in other studies they are assumed or fixed during simulation. This study also considered a good level of detail in simulation, going down to 90-minute time steps, and accounts for seasonal fluctuations using data from each month of the year. However, the location of DGs and the impact of DGs and EVs in the distribution system are not considered in this study.

The need for the inclusion of ESS in MGs to compensate for the intermittency of RES and provide storage and ancillary services to the grid is well documented above. Among the various different storage technologies,

batteries appear to be the front runner for an ESS in MGs (Katsigiannis et al. 2010). However, ESS batteries are expensive (Liu et al. 2018) and do not provide flexible capacity to accommodate and increased uptake in RES or increase in demand. To accommodate more RES and more demand in an MG, greater investment in ESS would be required, meaning potentially costly investments every decade.

An alternative that has not been considered by the research reviewed in this section is the use of the batteries present in EVs to provide the ESS services to the MG.

2.3 Electric Vehicles in Microgrids

In this section, the benefits of EVs in MGs are discussed as detailed in a prominent review by Mwasilu et al. (2014). Following this, the two predominant architectures for smart charging, centralised and decentralised control, are described and compared as reviewed by García-Villalobos et al. (2014). Finally, related works on both smart charging architectures are discussed and critically evaluated.

2.3.1 Integration of EVs in Microgrids

Batteries present in EVs have the potential to provide much value to an MG. Mwasilu et al. (2014) provided a comprehensive review of the use of EV batteries to provide services to the grid through V2G, citing the benefits as:

- Storage
- Peak shaving
- Ancillary services
- Load shifting

When using EV batteries as storage, energy produced by RES in times of high production, but low demand can be stored in EV batteries and later discharged when needed. Peak shaving occurs when energy from EV batteries is discharged to supplement unmet demand in times of low RES production (García-Villalobos et al. 2014). EV participation in peak shaving can be a prominent factor in maintaining energy autonomy from the upstream grid. Ancillary services include frequency control, load balancing and spinning reserve services (García-Villalobos et al. 2014).

Load shifting can be achieved through the control of EV charging. Smart charging strategies avoid the problem of uncontrolled charging whereby a large number of EVs charge at the same time due to people having similar daily routines. This often means that EV owners charge their cars after returning home from work in the evening. This leads to a surge in electricity demand on top of already peak demand times, putting a strain on supply, especially RES. Smart charging of EVs avoids this issue by scheduling charging patterns as to minimise peaks in demand.

2.3.2 Smart Charging of EVs

In a review of smart charging research by García-Villalobos et al. (2014), they state that two main control architectures have emerged: centralised control and decentralised control. The authors then describe and compare the two approaches. Centralised charging strategies involve a central controller that gathers data regarding EV charging demand, finds an optimal schedule in accordance with the charging objectives (such as minimisation of charging costs, flattening demand peaks or minimising emissions) and subsequently distributes an optimised charging schedule to each EV.

Centralised control provides a greater degree of control and is faster to respond to changes in demand and disruptions in the grid. On the other hand, a large communication infrastructure and powerful data processing capabilities are required to handle the large quantity of data needed. Depending on the size of the fleet being controlled, the optimisation problem can be very computationally intensive and this increases as the size of the fleet increases, meaning centralised control strategies have an issue with scalability. From a user perspective, consumers have become accustomed to being able to use as much electricity as they like at any time and so the adoption of such a strategy that restricts electricity use at certain times and limits the autonomy of the consumer will struggle to be adopted by users.

On the other hand, decentralised control distributes the optimisation problem to the EVs and influences the charging behaviour of EV owners through price signals. Each EV receives information about the price of electricity and finds an optimal charging schedule for that day that minimises

charging costs. Requests for electricity based on the schedule are then sent to the central control who balances the demand.

Decentralised control schemes are easier to implement because less communication infrastructure is required, there is less data to process making it less computationally intensive and it is more scalable than centralised schemes. However, it requires EVs to have the facility onboard to undertake the optimisation tasks which will increase the cost of already expensive EVs. It also can lead to a problem known as the avalanche effect. The avalanche effect occurs when many EVs schedule their charging to happen in the times of lowest cost due to them reaching the same optimal charging schedule. This also applies to discharging when there is a surge in supply from EVs due to favourable prices of selling electricity back to the MG.

2.3.3 Related Work

2.3.3.1 Decentralised Control

Dallinger & Wietschel (2012) developed an agent-based approach to control EV charging schedules using price signals in a grid with a high integration of RES. The goal of each agent, which are situated on the demand side, is to minimise the cost of EV chagrining. The charging behaviour is influenced through a pricing strategy in order to balance the intermittency of RES. Demand-side agents used a graph search algorithm to minimise charging costs in the 15-minute time period by optimising the charging schedule. The researchers use a stochastic approach to modelling driver behaviour, cal-

culating probabilities of travel on a certain day, the probability of starting a trip at time t on a given day, the probability of the distances travelled in the trip and the probability of the location of the destination (out of 4 possible). Probabilities are based on data from the "Mobility in Germany" travel survey. In addition, feedback of transformer utilisation is included to avalanche effects, whereby there is a sudden surge in vehicles charging or discharging at any one time due to favourable prices.

To test the approach the researchers constructed a scenario for Germany in 2030, using predicted data for electricity consumption and production and used the PowerACE simulation model to model the energy market. It was found that utilising EV batteries in this way improved the integration of RES into the electricity system and EVs provided a high power/energy ratio compared to pumped-storage hydropower used in Germany.

Ramachandran et al. (2013) design a MAS, consisting of EV agents, generator agents and load agents, main grid agent and optimising agent, with the goal of minimising the amount of energy taken from the upstream grid and the cost of energy production from DERs in the MG. The optimising agent uses an Artificial Immune System (AIS) algorithm to find the optimal power set points of EV charging/discharging and dispatchable DGs (micro-turbine and fuel cell) each hour, which are then communicated to the respective agents. Domestic loads fall into one of three categories: vital, non-vital and long term shut down. The domestic agent has the power to perform load shedding by shutting down its loads in priority order if there is not enough generated power to supply all loads.

It was found during simulation that when EVs were charging and domestic loads were at peak, the power generated in the MG in island mode was not sufficient to meet the demand. However, the proposed load shedding approach was successful in reducing the peak load and balancing generation and demand. This is a promising result for MGs with a high penetration for RES, however, the researchers only considered from 2 to 10 EVs in the MG. When 2 are present, no increase in peak load was found, and in the case of 10 EVs a small increase in peak demand was found. This indicates that as the number of EVs increase in the MG, the increase it will have on overall demand will increase exponentially, increasing the difficult of control and exacerbating the avalanche effect. At the level of EV penetration reviewed in this study, and with only a small increase in demand, the avalanche effect is not considered by the researchers. Also, this study does not consider V2G.

2.3.3.2 Decentralised Control

Saber & Venayagamoorthy (2011) used PSO to optimise the scheduling of DGs and EV discharging in order to reduce the cost and emissions of power systems. The variables to be optimised are the on/off state of each DG and the number of vehicles available to discharge to the grid each hour for a period of 24 hours. The cost objective function includes the cost of fuel, start-up and shut-down costs for DGs and the emissions objective function includes the cost of emissions for each DG. These are combined into a single objective function using weight coefficients. While the researchers found this method reduced costs and emissions by 1.1% when compared with a power system with no V2G, it is assumed that EVs are charged by RES but RES

output is not considered in the model. This assumption is unrealistic and does not account for the role of RES in the power system.

Tushar et al. (2014) propose a centralised control strategy to jointly optimising the scheduling of EV charging and home appliances to increase the reliability and stability of a MG while decreasing electricity prices to consumers. They formulate the model as a MILP which is solved using CPLEX. In their MG model, Markov chain state transition probability is used to predict the electricity generation output of WT and PV in the next 24 hours and the arrival and departure time of EVs is modelled using a Poisson process. The decisions variables in the model are the on/off state of home appliances, the charge/discharge state EVs and the amount of electricity imported from the grid in a given hour.

The model is compared to naïve strategy where there is no prior scheduling and a decentralised strategy based on a non-cooperative game. Results showed that the model led to a 175% improvement in performance over the naïve scheme and imported less energy from the grid on a daily basis compared to the decentralised strategy. The proposed model shows promising results and the comparison to the decentralised scheme is valuable.

Hu et al. (2019) used PSO to determine the optimal charge and discharge control strategies of EVs and thermal storage electric boilers for peak shaving. The objective function to be minimised is the standard deviation of the daily load curve. The charging or discharging power for each EV and boiler is determined for each hour in a 24-hour period. After optimisation, EVs and boilers are charged during low load periods and discharged during peak load

periods. It was found that increasing the number EVs and boilers in the simulation decreased the peak load incrementally. The researchers fail to consider seasonal variation or uncertainly in load profile as they only use load data from one day.

This paper presents a model for optimising the DER portfolio of residential MGs, incorporating the presence of EVs to aid in minimising the environmental impact of the MG and maximising the level of autonomy from the upstream grid through V2G services.

The proposed solution to optimising the capacity of DERs is the the Non-dominated Sorting Genetic Algorithm II (NSGA-II), a multi-objective evolutionary algorithm presented by Deb et al. (2002). NSGA-II has been selected because it is easy to adapt, it shows good performance compared to other MOEAs (Dougier et al. 2021) and has been widely used in this area of research.

The objectives for the optimisation of the mix and capacity of DERs are the Levelised Cost of Energy (LCOE) and the global warming potential of each of the DERs measured in kg CO2 equivalent/kWh through Life Cycle Analysis (LCA). LCOE is a benchmarking tool for comparing how costeffective different generation technologies are by estimating the cost of energy produced over the lifetime of a generating technology. It takes into consideration investment, operation, maintenance costs and residual value (IEA 2020). LCA establishes the emissions of a generating technology over its entire life including the emissions generated from the supply chain activities undertaken to create and transport the technology and the emissions gen-

erated in its decommissioning and disposal. Emissions are calculated in kg of CO2 /kWh, including the addition of equivalent CO2 produced for other GHG such as CH4 and N2O (Rillo et al. 2017).

Chapter 3

Methodology

The location of the MG to be optimised in this paper has been chosen as the town of Gogar, a few miles west of the City of Edinburgh. This is because it is a predominantly residential suburb making it a good site for a residential MG and it is located approximately 4.5 miles from Edinburgh city centre, which is in line with the average daily distance travelled for commuting in the UK. According to the National Travel Survey 2019 (DfT 2020) produced by the Department for Transport, people travelled on average 1,276 miles for commuting in 2019 across 140 trips on average, which is 9.1 miles per commute.

3.1 Experimental Set-Up

All code in this project was written in the Python programming language, specifically version Python 3.8.3 provided by the Anaconda distribution. The

Jupyter Notebook IDE was used to write all project code due to its benefits in rapid prototyping an interactivity which proved helpful in incremental simulation development.

In addition, a variety of Python libraries, packages and frameworks were utilised in this project which are summarised in Table 3.1.

Type	**Name**	**Use**
Library	NumPy	Data exploration, formatting and preparation
	Pandas	
	GeoPandas	
	Shapely	
	Matplitlib	
	SciPy	Statistical analysis and sampling from probability distributions
	NetworkX	Creating the special element of the EV simulation
Package	OSMnx	Downloading, extracting and formatting geospatial data used for EV simulation
Framework	Mesa	Creating Multi-Agent System used for MG simulation

Table 3.1: Python packages used in this paper

3.2 Microgrid Modelling and Simulation

In this paper, a Multi-Agent System (MAS) is used to model and simulate the proposed residential MG. In addition to this being a popular approach in the literature for modelling the Energy Management System (EMS) of MGs and EVs, MAS have been recognised as a promising control strategy in power engineering (Ramachandran et al. 2013).

The technologies used as DGs in this paper are PVs, WTs, Solid Oxide Fuel Cells (SOFC) and Lithium-ion Batteries; modelled using common modelling found in the literature. PVs and WTs have been chosen due to their widely known environmental benefits. SOFCs are power generators that convert chemical energy within fuel directly into electrical energy (Jiang et al. 2022). Specifically, SOFC has been chosen over other types of fuel cell such as a proton exchange membrane fuel cell (PEMFC) because of its high efficiency, easy maintenance, low pollution and it can be used with variety of fuels such as natural gas and biofuels (Fardadi et al. 2016). Also, in a techno-economic analysis comparing the performance of PEMFC to SOFC, Napoli et al. (2015) concluded that SOFC were preferable as a primary residential energy supply due to their high efficiency and low fuel consumption, making them a good candidate for a residential MG.

To capture the uncertainty in the output of RES, wind speed and solar irradiance will be modelled using the Weibull and Beta probability distribution functions (PDFs) respectively. The Beta distribution has been widely used in the literature to model solar irradiance (Samadi Gazijahani & Salehi (2017), Moghateli et al. (2020), Faraji et al. (2020)). The Weibull distribution is

used to model wind speed as research has shown that at a given location, wind speed is most accurately represented by this distribution (Hetzer et al. 2008) and it is has been used extensively in the literature (Aquila et al. (2016),Samadi Gazijahani & Salehi (2017),Moghateli et al. (2020), Faraji et al. (2020)).

Lithium batteries have been chosen as the BESS for the MG due to their long cycle life, high conversion efficiency, high energy density, high rated power and long discharge time compared to other available BESS (Wang et al. 2022).

In the following section, the modelling of DERs within the proposed MG will be detailed, including the mathematical models, descriptions of data used for these models and explanations of the processing steps undertaken on the data. Beginning with the modelling of residential loads before moving on to the DER component modelling.

3.2.1 Load Modelling

Apart from EVs, the loads in the proposed MG are all residential. Data to simulate these loads is taken from the IDEAL Household Energy Dataset produced by (Pullinger et al. 2021). Data is collected from 255 homes in Edinburgh and the Lothians and south Fife nearby in Scotland, UK over a 20-month period ending in June 2018 with a mean participation period of 286 days. 1-second apparent-power electricity data, pulse-level gas data, 12-second temperature, humidity and light data for each room and 12-second measurements of boiler pipe temperature are taken for each home. Additional

monitoring for 39 homes included plug-level monitoring of certain appliances, real-power of mains electricity monitoring and detailed heat and gas usage monitoring. The dataset can be downloaded in several zip files; one for documentation, one for metadata and one for sensor data. There are also additional zip files of data available for auxiliary data and appliance level monitoring.

The sensor data is contained in 1594 GZ files that can be read into a Pandas DataFrame with the help of an API provided by the creators of the IDEAL dataset. Due to the size of the dataset, with an average of over 30 million mains electricity readings for houses with a monitoring period of a year or more, the first step was to and reduce it.

To simulate the load profile of each house for each month for a full year, any houses that had a monitoring period of less than a year were removed. This reduced the dataset size from 250 houses to 60.

The mains electricity readings for each house, were read into Pandas DataFrames using the IDEAL API. Readings were once every second and measured in Watts. Each DataFrame was then re-sampled using the Pandas.DataFrame.resample function, specifying a sampling period of 1 hour by passing in 'H' as an argument and then chaining the Pandas.DataFrame.aggregate function, as shown in Figure 3.1. A lambda function was passed as an argument into the a Pandas.DataFrame.aggregate function that divided each value by 3600 to convert the value from Watt seconds to Watt hours, took the sum of each hour and divided by 1000 to convert to kilowatt hours (kWh). This further reduced the size of the dataset and made it computationally

more manageable with now an average of just over 11,000 reading per house.

```
def load_readings(houseid):
    'Funciton to load in data for the house electricity use'

    result = []

    data = ideal.get(homeid=houseid, subtype='electric-combined')[0]['readings']


    return data.size
```

Figure 3.1: Function to load IDEAL dataset mains electricity readings and re-sample to 1 hour

To prepare the data for the 24 simulation days, the average of each weekday and each weekend in every month was taken. To do this, a column was added to each of the resampled mains electricity readings DataFrames to numerically identify the day of the week, 0 for Monday through to 6 for Sunday. The algorithm described in Figure 3.2 was then used to format the data.

The starting month was chosen as January 2017, if the monitoring period for a particular house started after that time, the year was incremented so that the starting month was January 2018. From this point, the month was incremented by one after each iteration of the loop, however if a month was reached with no or incomplete data (indicating the end of the monitoring period), the years was decreased by one and the rest of the data taken from the previous year.

The weekday and weekend data is then split into 2 different DataFrames based on the value in the day identifier column. After this, the Pandas.DataFrame groupyby function is used passing in DataFrame.index.hour as an arguemnt to group all data by hour. The mean function is then called on this to take

the mean of each hour.

The aggregated weekday and weekend data for that month is then read into a Python dictionary and returned and the start and end month variables are incremeneted by 1 to aggregate the next months data.

Once this has been run on all houses in the sample data, the data is ready for the MG simulation.

3.2.2 Component Modelling

In the following section, the models used for simulating the DERs within the MG will be detailed along with the formatting and preparation of data used as their inputs during simulation.

3.2.2.1 PV Modelling

Monocrystalline PVs are used in this paper due to their increased efficiency over polycrystalline PVs (Ayadi et al. 2022). Specifically, the SunPower Maxeon 3 400W Solar Panel is used as the model system as it is one of the most efficient PVs currently available in the UK (Meyer 2022). Specifications for this system can be found in the datasheet depicted in Table 3.2 (SunPower 2022).

The output of each PV module is determined by the following model (Ogunjuyigbe et al. 2016):

$$P_t^{pv} = A_{pv} s_t \eta_{pv} \tag{3.1}$$

Table 3.2: Technical specifications of PV panels

Model	SPR-MAX3-400
Nominal Power	400W
Panel Efficiency Power	22.6%
Panel Dimensions (LxBxD) (mm)	1690 x 1046 x 40

Where P_t^{pv} is the output power of the PV module at time t in watts (W), A_{pv} is the area of the PV module in m^2, s_t is the global in-plane irradiance at time t in W/m^2 and η_{pv} is the panel efficiency.

Data Preparation

Data for the global in-plane irradiance is taken from the Surface Radiation Data Set - Heliosat (SARAH) - Edition 2.1 from Pfeifroth et al. (2017) and downloaded via the EU Commissions PVGIS 5.2 interactive tool (**?**). Data is downloaded in CSV format for the period 1 January 2005 to 31 December 2020 at point 55.936, -3.308 (latitude, longitude); the site of the "Home" node of the EV simulation as stated in section 3.2.

The global in-plane irradiance data is read into a Pandas DataFrame using the Pandas.read_csv method. As download, the column containing the date and time are in an incorrect string format of "YYYMMDD:HHMM". To use the date and time as the index of the DataFrame, a lambda function is applied to the column whereby the datetime string is reformatted to "YYYY-MM-DD HH:MM" and passed as an argument into Pandas.to_datetime to convert the date and time stored as a string into a datetime data type. This is then set as the index of the DataFrame.

The data is already in an hourly format, eliminating the need to resample the data, however it required reformatting in preparation for the simulation. To do this, a function was used whereby the hourly data for each day of each month of each year was read into separate DataFrames. A list of all DataFrames from each month was compiled, for example the list for January contained DataFrames for all January days from 2005 to 2020. These were then concatenated to make 12 DataFrames, one for each month of the year containing that months hourly data for each day of that month from the 16 year data period whereby the index is the day and year and the columns is the hours of the day as shown in Figure 3.3.

This structure readily enabled a Beta PDF (eq. 3.2) to be created based on the values of a single hour, considering all days of that month for 16 years, accounting for variation within the month and between years, accurately accounting for the variation in solar irradiance. The PDF of the Beta distribution is given by (Atwa et al. 2010):

$$f_b(s_t) = \frac{\Gamma(\alpha+\beta)}{\Gamma(\alpha)\Gamma(\beta)} s_t^{(\alpha-1)}(1-s_t)^{\beta-1} \tag{3.2}$$

Where s_t is the global in-plane solar irradiance at time t and α and β are the parameters of the Beta distribution and can be calculated using the mean (μ_{irr}) and standard deviation (σ_{irr}) as follows (Atwa et al. 2010):

$$\beta = (1-\mu_{irr})\left(\frac{\mu_{irr}(1+\mu)}{\sigma_{irr}^2} - 1\right) \tag{3.3}$$

$$\alpha = \frac{\mu_{irr}\beta}{1-\mu} \tag{3.4}$$

3.2.2.2 WT Modelling

The power curve of the SD6 Small Wind Turbine is used as the basis to calculate the output power of the WTs. Specifications for this system and for the EWT DW52 900kW WT for comparison of a larger system can be found in the datasheet depicted in Table 3.3 (SDWindEnergy (2022), EWT (2022)).

Table 3.3: Technical specifications of WTs

Model	SD6 Wind Turbine	DW52
Rated Power (kW)	5.2	900
Rated Wind Speed (m/s)	11	13
Cut In Speed (m/s)	2.5	3
Cut Out Speed (m/s)	None	25

The output of each WT at time t is determined by the following model (Hemmati (2017),Rakhshani et al. (2020), Faraji et al. (2020)):

$$P_t^{wt}(v_t) = \begin{cases} 0 & v_t < v_{ci} \\ P_{nom}\left(\frac{v_t - v_{ci}}{v_r - v_{ci}}\right) & v_{ci} < v_t < v_r \\ P_{nom} & v_r < v_t < v_{ct} \\ 0 & v_t > v_{ct} \end{cases} \tag{3.5}$$

Where v_t is the wind speed at time t in meters per second (m/s), v_{ci} is the cut-in wind speed of the WT, v_r is the rated wind speed of the WT, v_{ct} is the cut-out wind speed of the WT and P_{nom} is the rated power of the WT in kW.

The SD6 WT does not have a cut out speed and so output power remains constant at increasing wind speeds higher than the nominal wind seed.

Data Preparation

The wind speed data is exported in the same file, in the same hourly format as the global in-plane irradiance data as described in section 3.2.2.1. The processing and formatting required is the same as for the solar irradiance data described in section 3.2.2.1, resulting in the wind speed data, in m/s, having the structure as shown in Figure 3.3.

As stated in section 3.2, the Weibull distribution is used to model the hourly wind speed data to account for uncertainty in natural phenomena. The PDF is given as (Faraji et al. 2020):

$$f(v|k,\lambda) = \frac{k}{\lambda}\left(\frac{v}{\lambda}\right)^{k-1} e^{-(\frac{v}{\lambda})^k} \tag{3.6}$$

Where the shape (k) and scale (λ) parameters are estimated using (Faraji et al. 2020):

$$k = \left(\frac{\sigma_{wind}}{\mu_{wind}}\right)^{-1.086} \tag{3.7}$$

$$\lambda = \frac{\mu_{wind}}{\Gamma\left(1 + \frac{1}{k}\right)} \tag{3.8}$$

3.2.2.3 SOFC Modelling

The capacity of the SOFC is not set and is one of the decision variables of the NSGA-II algorithm. At the beginning of a simulation, the capacity of the SOFC in kW is passed as a parameter to the model. When used to generate electricity for the MG, the fuel consumption in £/kWh is calculated using (Chaouachi et al. 2013):

$$FC_t = C_t^F \frac{P_t^F}{\eta_F} \tag{3.9}$$

Where FC_t is the cost of the fuel consumed at time t, P_t^F is the output power of the SOFC in time t in kWh and η_F is the efficiency of the SOFC and C_t^F is the price of natural gas used. The price of natural gas is set at £0.054 /kWh, which is the average price of natural gas for consumers who used less than 278 MWh in the 1st quarter of 2022 (BEIS 2022). It is assumed that the price remains constant throughout the duration of the simulation.

The electric efficiency of the SOFC used in this paper is assumed to be 56%. This is the average of the efficiencies found by Cheng et al. (2019) for a SOFC system outputting from 1kW to 10kW and is in line with the efficiencies used in other studies on a range of system capacities (Elmer et al. (2015), Choi et al. (2019), Langnickel et al. (2020)).

The emissions output by the system are calculated using the following

equation, adapted from Elmer et al. (2015):

$$EM_t = \frac{P_t^F}{\eta_F}\varepsilon_{NG} \tag{3.10}$$

Where EM_t are the emmissions output by the SOFC in time t in kg(CO_2 eq.)/kWh and ε_{NG} is the natutal gas emissions factor in kg(CO_2 eq.)/kWh. In this paper, an emissions factor of 0.43 kg(CO_2 eq.)/kWh, taken from Rillo et al. (2017), is used.

3.2.2.4 Battery Modelling

As with the SOFC, the battery capacity is a decision variable of the optimisation algorithm and is entered as a parameter to the MG during simulation. The BESS is assumed to have an efficiency of 98% and its SOC is calculated using the following equation (Jiang et al. 2022):

$$SOC_{t+1}^B = \begin{cases} SOC_t^B + P_t \frac{1}{\eta_b} \frac{\Delta_t}{E^B} & \text{charging} \\ SOC_t^B - P_t \eta_b \frac{\Delta_t}{E^B} & \text{discharging} \\ SOC_t^B & \text{idle} \end{cases} \tag{3.11}$$

Where SOC_{t+1}^B is the SOC of the BESS at time $t+1$, SOC_t^B is the SOC of the BESS at time t, P_t is the input or output power of the BESS at time t, η_b is the BESS efficiency, Δ_t is the chang in time t in hours and E^B is the capcity of the battery in kWh.

Constraints

Fully discharging the BESS can have negative impacts on the life span of a battery, therefore, the depth of discharge is limited to 90% (Chowdhury et al. (2020), Wang et al. (2022)) using the constraint:

$$10\% \leq SOC_t^B \geq 100\% \tag{3.12}$$

3.2.2.5 EV Modelling

The EV modelled in this paper is the Tesla Model 3, which has been chosen as it is the most registered battery EV in the UK in 2022 (DfT 2022). The battery parameters of the EV is provided in Table 3.4 (ElectricVehicleDataBase 2022). The Tesla Model 3 currently comes in 2 range options, the standard range with a battery capacity of 60kWh and long range with a capacity of 75 kWh. The long-range model with a 75kW has been chosen for simulation as it is in line with future trends in battery capacity of 70-80kWh (IEA 2019).

Table 3.4: Technical specifications of Tesla model 3

Model	Tesla Model 3 Long Range Dual Motor
Battery Capacity (kWh)	75
Range (miles)	280
Efficiency (kWh/mile)	0.25

The amount of energy stored in the battery at the end of each hour is given by eq. 3.13(Rabiee et al. 2016):

$$E_t^B = E_{t-1}^B - P_{trip,t} + \Delta_t \left(\eta_c P_{ch,t} - \frac{1}{\eta_d} P_{Dch,t} \right) \tag{3.13}$$

Where E_t^B is the energy stored in the battery at the end of hour t, Where E_t^B was the energy stored in the battery in the previous hour $t-1$, $P_{trip,t}$ is the power used by the EV by any trips taken in hour t in kWh, Δ_t is the change in time t in hours, $\eta_c P_{ch,t}$ and η_d are the charging and discharging efficiency, $P_{ch,t}$ is the amount of charge given in hour t in kWh and $P_{Dch,t}$ is the amount discharged in hour t in kWh. The charging and discharging efficiency is assumed to be 92% (O'Neill et al. 2022).

Constraints

To minimise EV battery degradation, the SOC is kept within a range (Tan et al. 2016):

$$20\% \leq SOC_t^V \geq 80\% \tag{3.14}$$

Where SOC_t^V is the SOC of an EV at time t.

3.3 Multi-Agent System

In this section, the details of the MAS will be presented, detailing the agents, the algorithms within them and the interactions between them. In particular, the strategies used by the Control Agent to balance the power within the MG and optimise EV charging and discharging will be explained.

As stated in section 3.2, a MAS is used to evaluate the performance of

MG during optimisation. The MAS is built using Mesa, an agent-based Python framework (Kazil et al. 2020). This was chosen due to the flexibility of the spatial component of the framework that enabled the integration of an EV simulation within the MAS using custom spatial and geospacial data. Simulating the EVs in this way allowed for more realistic driver behaviour over hard-coding trips and is based a study by Marmaras et al. (2017) who created an integrated, MAS-based simulation to modelling EVs and their interactions and impact in road networks and electric power systems.

The MAS is made up of 3 primary components; model, agent and spatial. The model class handles the MAS at a global level, holds model level data and attributes and manages the agents. There are 6 agent classes a BESS Agent, a RES Agent, a Residential Load Agent, an EV Agent, an EV Aggregator Agent and a Control Agent. The agent classes contains the agent level data, attributes and algorithms used by the agents to interact with other agents and their environment. The spatial class contains the spatial data of the space the agents exist in and handles the moving of agents around the space during simulation.

3.3.1 Model

The model takes as inputs; the number of EVs, the number of PV panels, the number of WT, the capacity of the SOFC in kW, the capacity of the battery in kWh. These are then set as model level attributes. The model also takes as inputs a DataFrame containing the solar data, a DataFrame containing the wind speed data, a DataFrame containing the residential load

data, the graph used for the spatial element and a dictionary of activities the EV owners can chose from, which are all set as model level attributes.

The agents are then created by instantiating instances of each agent class. For the EVs, each EV agent represents 1 EV, so the number of EV agent classes instantiated is equal to the number of EVs passed as an input into the model.

Time in the MAS is simulated in steps where each step represents 1 hour. In Mesa, the scheduler model component is used to control the order in which agents are activated in each step. The BaseScheduler is used in which the agents are activated in the order that they are added to the scheduler. The BESS agent is added first, then the RES Agent, the Residential Load Agent, the EV Agents, the EC Aggregator Agent and finally the Control Agent. The Control Agent is added last as it must wait to receive data from all agents before running its control strategies.

The scheduler stores the agents in a list which can be accessed by the model and all agents. If an agents wants to interact with another agent of the same or different type, they can do this by finding the desired agent in the scheduler.agents list and calling the necessary method within that agent.

The step function of the model class calls the scheduler which activates the step function of each agent in the order they were added to the scheduler. To simulate the months, days and hours, 3 for loops are used. The first iterates through a range of months, in each iteration, a for loop its created with a range of 2, 1 for the weekday and 1 for weekend days to be simulated. Within this, a for loop with a range of 24 is created to simulate the current day, 1

iteration representing 1 hour. The scheduler then calls the step function of each agent in each iteration.

3.3.2 Space

The spatial component of the MAS represents a geographical region containing a road network that the EVs move around throughout the simulation. In Marmaras et al. (2017), the nodes of the network were districts that contain destinations for the EVs such as work, leisure or home.

This functionality is possible thanks to the spatial component of Mesa that allows users to create three types of space. A SingleGrid, a square grid the allows only one agent per cell at a time, a MultiGrid, a square grid that allows multiple agents in a cell at a time and a NetworkGrid, a graph of any shape containing nodes and edges. In this paper a NetworkGrid is used because it is the most flexible and representative of a road network.

NetworkGrids can be created using NetworkX (Hagberg et al. 2008), a Python package for studying graphs and networks. As stated at the beginning of this chapter, the proposed location for the MG is in Edinburgh, Scotland, therefore the NetworkGrid is modelled on the Edinburgh road network. To do this, the geospatial data of the Edinburgh road network is downloaded using the OSMnx Python package (Boeing 2017) which enables users to download geospatial data from OpenStreetMaps. The OSMnx.graph_from_place function is used passing in 'Edinburgh, Scotland' and network_type='drive' as arguments. This function downloads the geospatial data and creates a NetworkX MultiDiGraph, a directed graph that can accommodate multiple

edges between nodes.

The nodes in the MultiDiGraph created are junctions and the edges are the roads between them. Using the OSMnx.distance.add_edge_lengths function, the length of each road is added as an attribute to its respective edge. The MultiDiGraph is then saved locally as a graphml file.

Supplementary data regarding the nodes and edges can be stored in GeoPandas (Jordahl et al. 2020) GeoDataFrames using the OSMnx.graph_to_gdfs function and passing in the MultiDiGraph as an argument. There are 13318 nodes and 30717 edges in the Edinburgh road network MultiDiGraph.

To define destinations in the graph for the EVs, 30 coordinates for work and 20 for leisure were randomly chosen around Edinburgh city centre. The closest node to each of these points was then identified by using the Shapely Python package (Gillies et al. 2007–). Each of the proposed destination coordinates was converted into a shapely.Point data type to match the nodes which were already in this datatype. The distance was then measured between each node and each point using the shapely.Point.distance and stored in the GeoDataFrame containing the nodes. The closest node to each destination Point was then assigned as that destination and its type attribute of either “work” or “leisure” given. All other nodes were given the attribute “other”. Figure 3.4 shows the location of ”work” nodes and figure 3.5 shows the locations of the ”leisure” nodes around Edinburgh.

To give the nodes attributes, a Phython dictionary was created where the keys were the node identifiers provided by OSMnx and the values were the type attributes as strings. These are then applied to the nodes using

NetworkX.set_node_attributes and passing in the MultiDiGraph of the Edinburgh road network and the dictionary of node : attribute pairs.

3.3.3 Agents

When instantiated, all agents create attributes for the month, day and hour which are created using the model attributes for the same value. For each agent, when the step function is called the first thing that happens is these parameters are updated.

3.3.3.1 Residential Load Agent

After updating the month, day and hour parameters the Residential Load Agent updates the load data currently stored by the agent by calling the data stored in the model using the month, day and hour as parameters to get the cut of data relevant to that time step.

The sum of the load demand of each house for hour t is then taken by iterating through the houses in the data structure using a for loop. The total residential load is then sent to the Control Agent.

3.3.3.2 RES Agent

When the RES Agent is instantiated by the Model, it initiates the parameters of the PVs and WTs presented in Table 3.2 and 3.3 respectively, in addition to setting the number of each which are design parameters set during optimisation.

When the step function is called by the scheduler the RES Agent updates the historic solar and wind data by calling the data stored in the model using the month, day and hour as parameters to get the cut of data relevant to that time step. The value for the solar irradiance and the wind speed are then calculated.

Solar Irradiance Value

The cut of historic solar irradiance data for the current time step is first normalised using min-max normalisation given in eq. 3.15.

$$x_{norm} = \frac{x - x_{min}}{x_{max} - x_{min}} \tag{3.15}$$

Where x is the value pre-normalisation, x_{norm} is the normalised value, x_{min} is the lowest value in the sample and x_{max} is the highest value in the sample.

The mean and standard deviation of the normalised data are then calculated using NumPy.mean() and NumPy.std() from the NumPy library. Using these values, the beta and alpha parameters of the Beta distribution are calculated using eq. X. A random variable is then sampled from the Beta distribution produced using the alpha and beta parameters using the r scipy.stats.rv_continuous.rvs() method with Beta as the rv_continuous distribution.

Wind Speed Value

The mean and standard deviation of the historic wind speed data are calculated using NumPy.mean() and NumPy.std(). Using these values, the shape and scale parameters of the Weibull distribution are calculated using

eq. X. A random variable is then sampled from the Weibull distribution produced using the alpha and beta parameters using the r scipy.stats.rv_continuous.rvs() method with Weibull as the rv_continuous distribution. The output of the PVs and WTs is calculated using eq. and eq. respectively, inputting the solar irradiance and wind speed random variables as parameters. The amount of energy generated by the RES is then sent to the Control Agent.

3.3.3.3 BESS Agent

In addition to this, the function to update the SOC is contained within the BESS Agent. The Control Agent can charge and discharge the BESS by calling this function and passing in the desired energy as an argument. If the argument value is positive, the battery is charged using eq. X, if it is negative, the battery is discharged using eq. X

If the desired charge or discharge exceeds the limits specified by constraint X, the surplus power after charging or discharging the BESS to its maximum upper or lower limit is calculated using:

$$P_t = \frac{SOC_x - SOC_y}{1} E^B \eta_b \tag{3.16}$$

This then subtracted from P and the SOC is updated with the correct amount. The surplus power is then returned from the function so that the Control Agent is aware if there is still a surplus or a deficit in power.

3.3.3.4 EV Agent

If the time step t is equal to 0 (midnight) when the step function is called, the EV Agent first performs a check on the location of the EV, if it is not at "Home", it is moved to the home node. It is assumed in this paper that the EVs are all following a pattern of normal daily use for example commuting and recreational activities and so it is reasonable to assume that all EVs will be home by midnight. The EV then creates its list of activities to undertake in that day of simulation. This approach is based on a study by Marmaras et al. (2017) who created an integrated, MAS-based simulation for modelling EVs and their interactions and impact in road networks and electric power systems. In their approach, at the beginning of each day, each EV chose between 3-5 activities from a predefined list that would be in effect their owners schedule for the day.

In this paper, when the daily list of activities is being created, a random number is first chosen from a range of 3-5 using numpy.random.choice(numpy.arrange(3,6)). A list of this size is then created where activities from the predefined list of activities are chosen based on a probability distribution. It is assumed that most of the trips taken by EV owners in the MG are commuting trips therefore the work-related activities have a higher probability compared to the leisure activities as shown in Table 3.5. Each activity also has a duration that is the number of hours that activity will take before the EV moves to its next activity or home. Each EV is limited to 10 hours of activities a day.

One the day's activities have been chosen, the time for the EV to leaving "Home" in the morning is decided. It is widely known that the majority

of people with office-based jobs generally leave for work between 6am and 9am, therefore a value is chosen between 6 and 9 (inclusive) with along a probability distribution of 0.15 for 6 and 9 and 0.35 for 7 and 8. This ensures it is more likely the EV will leave at 7am or 8am, in line with rush hour times. If time t = the leaving time, then the Boolean move variable is set to true.

At each time step, a check is performed to determine if the EV is able to charge or discharge. The conditions for charging and discharging are shown in X. If a condition is met, the corresponding charge or discharge bool variable is set to true, otherwise they remain false and the EV is idle.

If either the charging or discharging variable are true, the EV sends its SOC to the EV Aggregator Agent to register for charging or discharging.

Table 3.5: Activities available to the EV Agent

Type	**Name**	**Time (hours)**	**Probability**
Work	Work1	4	0.3
	Work2	3	
Leisure	Sport	2	0.08
	Shopping	2	
	Food	1	
Other	other	1	

Trips

The Boolean move variable is checked each time step. If it is true and the

EV has completed all activities in its daily activity list, the next destination is set to "Home", otherwise the next destination is set to the next activity in the list. Once the next destination is set, the first step is to find a not in the graph of that type.

1. Find destination node:

   A list of all nodes in the graph of the correct type is created using a for loop to iterate through the nodes of the graph and adding them to the list of their "type" attribute matches the activity type. Then, one of the nodes from this list is chosen at random as the next destination.

2. Get path

   The route to the next destination represented by the shortest path through the graph to the destination node is calculated using the NetworkX.shortest_path method, where the graph, source and target nodes are given as arguments. By default this uses Dijkstra's algorithm to determine the shortest path.

3. Calculate distance

   To calculate the distance travelled by the EV from its starting node to the destination, the path list created from step 2 is iterated through and the weight attributes of the edges, which are the road lengths added during the creation of the MultiDiGraph as described in section 3.3.2, are totalled.

4. Update SOC

After the trip, the SOC of the EV is updated using eq. 3.13. The power used during the trip is calculated by multiplying the distance travelled in miles and the efficiency of the EV described in Table 3.4.

The agent level location variable is also updated to the new location and the activity time variable is updated to be the time associated with the current activity. Regardless of whether the agent has moved within the time step, the activity time is reduced by 1. If it is equal to 0, the Boolean move variable is set to true and the agent will move to its next destination in the next time step.

3.3.3.5 EV Aggregator Agent

The role of the EV Aggregator Agent is to be the mid-point between the EVs and the Control Agent. At each time step, all EVs that want to charge or discharge register with the EV Aggregator Agent which pools the charging and discharging demand and sends the information to the Control Agent. The EV Aggregator compiles a Python dictionary where the keys are the ids of the EVs that have registered during the time step and the values are objects containing the SOC of that EV and the energy demand in kWh if the EV is registered to charge.

3.3.3.6 Control Agent

The Control Agent acts as the Energy Management System (EMS) for the MG, responsible for balancing the supply and demand of energy and optimis-

ing the charging and discharging of EVs. First, the Control Agent calculates the current energy balance using the following eq.

$$P_t^{mg} = P_t^{pv} + P_t^{wt} - P_t^{res} - \sum_{i=1}^{n} P_{i,t}^{ev} \tag{3.17}$$

Where P_t^{res} is the total residential load demand in hour t in kW and the sum of $P_{i,t}^{ev}$, the charging demand of EV i in time t in kW, is taken for all charging EVs n.

If the value is negative, there is a surplus of energy form the RES and this is fed to the BESS. If the BESS is currently at maximum capacity according to constraint 3.12, the surplus is sold to the upstream grid. If the value is positive, there is a deficit where demand is exceeding supply and the Control Agent initiates a number of strategies in an attempt to meet this excess demand. The control strategies are executed in the following order:

1. BESS

   The Control Agent uses the SOC information sent by the BESS agent to determine if the deficit can be met using the BESS. If so, the necessary amount of energy is taken from the BESS and the SOC updated. If not, the Control Agent discharges the battery to its maximum allowed limits as defined in constraint 3.12 and updates the deficit to be the remaining demand not met by the BESS.

2. V2G

   If after discharging the BESS there is still a deficit, the Control Agent discharges the EVs registered to discharge. This is optimised using Par-

ticle Swarm Optimisation (PSO) and implemented using the PySwarms library. The aim of the optimisation to find the optimal charge set points for each of the EVs registered for V2G so that the deficit is met (if possible) and the charge taken from each EV is proportional to it's SOC. The objective function to be minimised is:

$$\min(|d - P_t^{v2g}| + Var(SOC_t) \tag{3.18}$$

Where d is the demand to be met, $P_{i,t}^{v2g}$ is the proposed V2G power of EV i at time t and $Var(SOC_t)$ is the variance of the SOC of all EVs registered for V2G. By minimising the variance not EV gets a disproportionate amount taken from their battery in the time period.

3. SOFC

   If there is still a deficit in demand to be met, the Control Agent then uses the SOFC. The fuel cost of running the SOFC is determined by eq. X where P is the remaining demand deficit. If the capacity of the SOFC is less than the deficit, the deficit is updated the be the remaining demand after running the SOFC at maximum capacity. The emissions are also calculated.

4. Grid

   Any remaining deficit in demand is then met by the grid.

If at any point during the dispatching of the control strategies there is a surplus, this is used to charge the BESS and any remaining is sold to the grid.

3.4 Optimisation

As stated in section 2.3, the optimisation of the MG design parameters is performed using NSGA-II. In the following section the objectives and constraints used during optimisation will be detailed in addition to explanations as to how they were implemented. Then, the values of operators used during optimisation will be summarised alongside rational as to their choice. Finally, the testing scenarios will be summarised.

3.4.1 Objectives

The objectives of the NSGA-II in this paper are to minimise the LCOE and GHG emissions based on LCA, calculated after a candidate MG has been simulated using:

$$LCOE = \sum_{t=0}^{n} C^{pv} P_t^{pv} + C^{wt} P_t^{wt} + C^{fc} P_t^{fc} + CS^B SOC_t^B + C^g P_t^g \quad (3.19)$$

Where t is the hour up to n the total number of hours of simulation, C is the LCOE value for that energy resource, CS is the LCOES for the BESS, P_t^g is the power from the upstream grid.

$$LCA = \sum_{t=0}^{n} EM^{pv} P_t^{pv} + EM^{wt} P_t^{wt} + EM^{fc} P_t^{fc} + EM^B SOC_t^B + EM^g P_t^g \quad (3.20)$$

Where t is the hour up to n the total number of hours of simulation, EM

is the LCA value for that energy resource.

Therefore the objective of the NSGA-II optimisaiton are:

$$\min(LCOE) \tag{3.21}$$

$$\min(LCA) \tag{3.22}$$

In addition to these objectives, the optimisation will be run using the amount of energy the MG buys from the upstream grid as a constraint. This will ensure that all candidate solutions are stand-alone MGs and do not draw power from the gird. The effect this has on solutions will be reviewed.

3.4.2 Design Space

To limit the size of the design space, an upper bound is put on each of the design variables. The upper bounds have been determined based on reasonable assumptions about the space within the MG to accommodate these technologies and the energy requirement of the MG. The number of PV panels has been limited to 500, which at its upper bound would equate to approximately 10 panels per household. The number WTs is limited to 150 as it is approximately equivalent to 3 per household. Alternatively, 150 6kW WTs is equivalent in terms of capacity to a single 900 kW WT, which has the same LCOE and LCA values and is comparable in terms or technical specifications as compared in Table 3.3. The upper bounds of the SOFC and Battery are based on average total daily load. On average the demand of the

residential load data used in the simulation is 549.7 kW therefore the upper limit on SOFC and BESS capacity is 550.

All design variables have a lower bound of 0 to allow the algorithm to omit specific DERs from the MG design.

3.4.3 Operators

To choose the appropriate operators for the NSGA-II, namely population size, number of generations, crossover and mutation probability, tests were carried out and the most promising operator values chosen.

Population Size

The algorithm was run for 50 generations with population of 50, 100 and 200 to analyse the effect of population size on the output of a set of optimal solutions. Running the algorithm with a population size of 100 produced the highest variety in solutions with 14 non-dominated solutions after 50 generations, whereas a population size of 50 produced 11 and 200 produced 5. Therefore, population size was chosen to be 100.

Generations

The algorithm was run for with a population of 100 with generations of 30, 80 and 100 to analyse the effect of population size on the output of a set of optimal solutions. A population size of 100 for 50 generations had already been tested in the population test. Running the algorithm for 30 generations resulted in 20 non-dominated solutions, 80 generations produced 9 and 100 produced 13. As 30 generations produced the highest number of

non-dominated solutions, it has been chosen as the number of generations.

Crossover, mutation and repair

Values for crossover and mutation were taken from Morvaj et al. (2016) and are summarised in Table 3.6. Due to the size of the design space and the design parameters being integers, the design variables were discretised using the Pymoo RoundingRepair function.

Table 3.6: NSGA-II Operators

Population	100
Generations	30
Crossover	0.9
Mutation	0.5

3.4.4 Implementation

To implement this optimisation in Pymoo, the problem needs to be defined. This is done by creating a custom problem class which is a subclass of Pymoo Problem. Pymoo is inherently parallelised for efficiency, however, due to the evaluation of candidate solutions being a sequential simulation, the ElementwiseProblem superclass was used instead. This enables the candidate solutions to be evaluated 1 at a time.

When instantiating the custom problem, the parent ElemenwiseProblem is instantiated with the number of design variables, the number of objectives, the number of equality constraints (if any), the number of inequality

constraints (if any) and the upper and lower bounds of the design space.

Each candidate solution was an array containing the number of PVs, number of WTs, capacity of SOFC and capacity of BESS. When the Pymoo _evaluate function is called to evaluate the current set of solutions one at a time, the design parameters are first extracted from the array before being used to instantiate a MicrogridModel. The MicrogridModel's step function is then called and the simulation is run. Thhe LCOE and LCA value of the proposed solution is then calculated and stored in the output array. The custom problem clas is shown in figure 3.6.

3.4.5 Testing scenarios

Due to a very high computation time when running with 24 days of simulation, the NSGA-II optimisation is run using MG simulations based on 4 days, using the average days load data for each season. After outputting the optimal set, a selection of the solutions will be run on the full simulation to assess the viability of the solutions and view the energy balances. In addition, the full Edinburgh road map is use for the simulation after optimisation due to computational time. One run of the simulation with the full road network take approximately 100 seconds which does not work for the optimisation algorithm. Instead a small undirected graph with 10 nodes is utilised where the weights simulate the distances travelled by the EVs in the full Edinburgh road netowrk. After testing it was confirmed the out come for the EVs was similar but computation time was much quicker.

The model will be tested using 3 scenarios of EV penetration in the MG.

To be representative of the current penetration of EVs in the UK which is less than 1% (DfT 2022), scenario 1 was set to be 1 EV, however this produced results not significantly different enough from the control scenario and so scenario 1 contains 10 EVs, the second will contain 30 (50% penetration) and the third will contain 45 (75% penetration). These scenarios will demonstrate how the MG design algorithm responds to different levels of EV presence in the MG. In addition, a control scenario will be tested where no EVs are present to provide a baseline as to the MG behaviour in the presence of no EVs.

```
def aggregate_days(data):
    'Function to take the average data for each hour of all weekdays and weekends'

    'Initiate first and last days of the month as datetime'
    startdate = datetime.datetime(2017, 1, 31)
    enddate = datetime.datetime(2017, 1, 31)

    'Create empty dictionary to contain result'
    result = {}

    'If the first day in the dataset is after 1/1/2017, make start date 1/1/2018'
    if data.index.min() > startdate:

        startdate = datetime.datetime(2018, 1, 1)
        enddate = datetime.datetime(2018, 1, 31)
    else:

        startdate = datetime.datetime(2017, 1, 1)

    'Iterate through 12 months and aggregate weekday and weekend data'
    for i in range(12):

        'Get one month cut of the data using start and end dates of month'
        df_cut = get_cut(data, startdate, enddate)

        'Seperate weekday and weeekend data into different DataFrames'
        weekday = df_cut.loc[df_cut['day'] < 5]
        weekend = df_cut.loc[df_cut['day'] > 4]

        'Remove the day identifier column'
        weekday.drop('day', axis=1, inplace=True)
        weekend.drop('day', axis=1, inplace=True)

        'Group all data by hour and take the mean of each hour'
        weekday = weekday.groupby([weekday.index.hour]).mean()
        weekend = weekend.groupby([weekend.index.hour]).mean()

        result[i] = {0: weekday, 1: weekend}

        'Move to next month'
        startdate = increment_month(startdate)
        enddate = increment_month(enddate)

    return result
```

Figure 3.2: Function to aggregate the each months weekends and weekdays by the mean of each hour

	0	1	2	3	4	5	6	7	8	9	...	14	15	16	17	18	19	20	21	22	23
2005-01-01	0.0	0.0	0.0	0.0	0.0	0.0	0.0	0.0	0.0	0.00	...	9.03	3.61	0.00	0.0	0.0	0.0	0.0	0.0	0.0	0.0
2005-01-02	0.0	0.0	0.0	0.0	0.0	0.0	0.0	0.0	0.0	0.00	...	126.70	13.55	0.00	0.0	0.0	0.0	0.0	0.0	0.0	0.0
2005-01-03	0.0	0.0	0.0	0.0	0.0	0.0	0.0	0.0	0.0	0.00	...	9.03	6.32	0.00	0.0	0.0	0.0	0.0	0.0	0.0	0.0
2005-01-04	0.0	0.0	0.0	0.0	0.0	0.0	0.0	0.0	0.0	0.00	...	417.75	187.25	0.00	0.0	0.0	0.0	0.0	0.0	0.0	0.0
2005-01-05	0.0	0.0	0.0	0.0	0.0	0.0	0.0	0.0	0.0	0.00	...	9.03	317.68	0.00	0.0	0.0	0.0	0.0	0.0	0.0	0.0
...	...	...	...	...	...	...	...	...	...	...	...	...	...	...	...	...	...	...	...	...	...
2020-01-27	0.0	0.0	0.0	0.0	0.0	0.0	0.0	0.0	0.0	26.78	...	600.27	357.68	0.00	0.0	0.0	0.0	0.0	0.0	0.0	0.0
2020-01-28	0.0	0.0	0.0	0.0	0.0	0.0	0.0	0.0	0.0	27.62	...	493.49	125.63	0.00	0.0	0.0	0.0	0.0	0.0	0.0	0.0
2020-01-29	0.0	0.0	0.0	0.0	0.0	0.0	0.0	0.0	0.0	158.96	...	30.71	18.97	0.00	0.0	0.0	0.0	0.0	0.0	0.0	0.0
2020-01-30	0.0	0.0	0.0	0.0	0.0	0.0	0.0	0.0	0.0	28.63	...	204.23	101.72	2.71	0.0	0.0	0.0	0.0	0.0	0.0	0.0
2020-01-31	0.0	0.0	0.0	0.0	0.0	0.0	0.0	0.0	0.0	39.95	...	107.93	72.85	4.52	0.0	0.0	0.0	0.0	0.0	0.0	0.0

Figure 3.3: DataFrame structure of global in-plane solar irradiance and wind speed data.

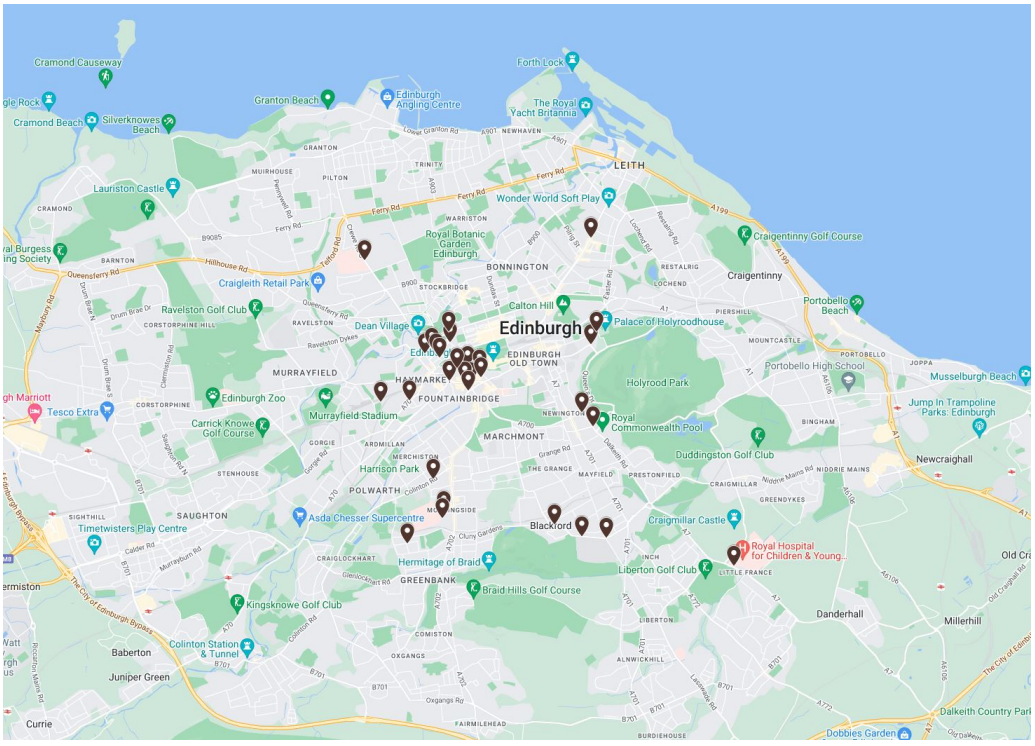

Figure 3.4: Locations of work nodes in the Edinburgh road network

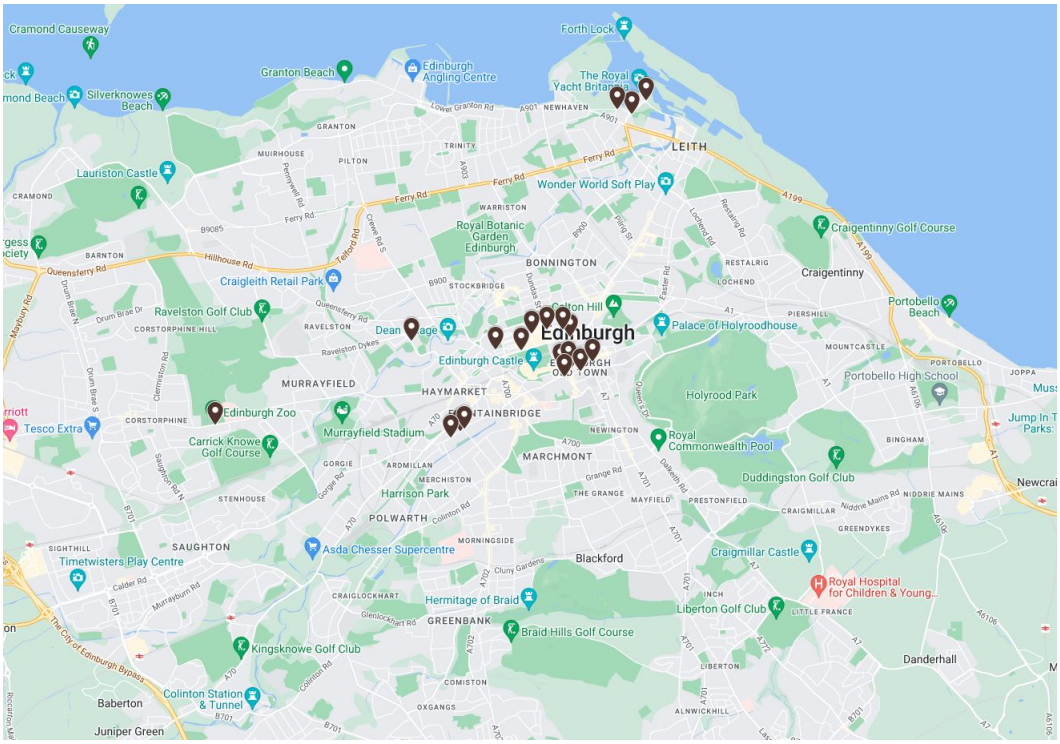

Figure 3.5: Locations of leisure nodes in the Edinburgh road network

```
class MicroGridProblem(ElementwiseProblem):

    def __init__(self, evs):
        super().__init__(n_var=4, n_obj=2, xl=0.0, xu=np.array([100,150,500,500]))
        'Initiate number of EVs in simulation'
        self.evs = evs

    'Calculate the LCOE of a proposed MG solution'
    def calculate_cost(self, mg, bess_cap):
        solar_gen = mg.get_solar_gen()
        wind_gen = mg.get_wind_gen()
        fuel_cell = mg.get_fc_use()
        bess_cost = mg.get_bess_charges()
        grid_cost = mg.get_grid_price()

        solar_total = self.sum_dict(solar_gen)
        wind_total = self.sum_dict(wind_gen)
        fc_total = self.sum_dict(fuel_cell)
        bess_total = bess_cap*self.sum_dict(bess_cost)
        grid_total = self.sum_dict(grid_cost)/100

        solar_total *= 0.2076275
        wind_total *= 0.046
        fc_total *= 0.23
        bess_total *= 0.25
        grid_total *= 0.3

        return np.sum([solar_total, wind_total, fc_total, bess_total, grid_total])

    'Calculate the LCA of a proposed MG solution'
    def calculate_emmissions(self, mg, bess_cap):
        solar_gen = mg.get_solar_gen()
        wind_gen = mg.get_wind_gen()
        bess_cost = mg.get_bess_charges()
        grid_gen = mg.get_grid_use()

        solar_total = self.sum_dict(solar_gen)
        wind_total = self.sum_dict(wind_gen)
        fc_total = self.sum_dict(fc_ems)
        grid_total = self.sum_dict(grid_gen)
        bess_total = bess_cap*self.sum_dict(bess_cost)


        solar_total *= 0.2076
        wind_total *= 0.2240
        bess_total *= 0.054
        grid_total *= 0.228
        fc_total *= 0.43

        return np.sum([solar_total, wind_total, fc_total, bess_total, grid_total])

    'Function to get the total of the values of a particular metric output from the simulation'
    def sum_dict(self, obj):

        return np.sum(np.fromiter((np.sum(np.concatenate(list(np.array(list(obj.values()))[i]
                                                              .values())))) for i in list(obj)),float))


    'Evaluate the candidate solutions'
    def _evaluate(self, x, out, *args, **kwargs):
        panels = x[0]
        turbines = x[1]
        fc_cap = x[2]
        bess_cap = x[3]
        mg = MicrogridModel(self.evs, panels, turbines, fc_cap, bess_cap, solar_data, wind_data, df,
                            G, activities, grid_prices)
        mg.step()
        cost = self.calculate_cost(mg, bess_cap)
        em = self.calculate_emmissions(mg, bess_cap)
        grid_gen = mg.get_grid_use()
        grid_total = self.sum_dict(grid_gen)
        out["F"] = [cost, em] # Objectives
        out["G"] = grid_total # Constraints
```


Figure 3.6: Problem class defined for Pymoo NSGA-II

Chapter 4

Results and Discussion

In the following section the results of the testing described in section 3.4.5 are presented and critically evaluated. Certain optimal solutions from each scenario will be simulated using the 12 month simulation containing the Edinburgh road network to evaluate in more detail the performance of the MG using the proposed design parameters.

This will be followed by a reflection on the aims and objectives of the study and a critical evaluation as to whether they have been met. The study limitations and their implications will also then be discussed.

4.0.1 Results

4.0.1.1 Control Scenario

Figure 4.1 displays the optimal set of solutions after 50 generations with no EVs present in blue. While there is no pre-defined Pareto optimal front for this problem, there is a good distribution of solutions along the front produced and there is little deviation away from the front, indicating a good diversity in solutions and the set produced is close to optimal if not optimal. The highest emissions and lowest cost with an LCOE value of £74.80 and LCA value of 1171 was a solution that relied solely on the grid and did not implement any of the DERs in the design space. The solution with the highest cost and lowest emissions had and LCOE value of £409 and LCA of 756 was a MG with a 120 kW SOFC but no other DERs. In the middle of the front with an LCOE of £226.35 and LCA of 990 was a solution that implemented 11 WTs and a 9kW SOFC.

Figure 4.1 displays the optimal set of solutions in red after 50 generations with no EVs present with the constraint that no energy be purchased from the grid. The solutions are noticeably more expensive with the cheapest having a LCOE of £237.12 when compared with £74 without the constraint. This is consistent with the input data as the cost of buying energy from the upstream grid does not exceed £0.19 over the course of the day whereas the LCOE of the DERs are mostly above £0.2. The LCA values are also higher, which can be attributed to the presence of larger SOFCs in order to keep the grid autonomous, however SOFCs have the highest LCA out of the available energy options. The middle of the front is also higher with LCOE of £317.59

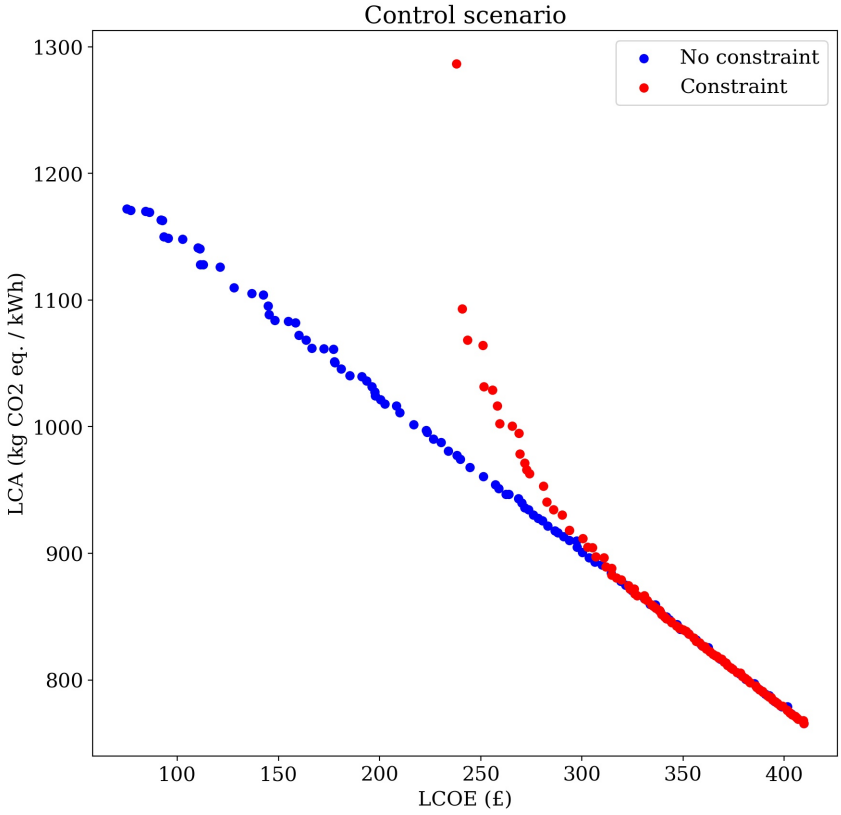

Figure 4.1: Control scenario results set

and LCA of 880. This solution uses 1 PV, 25 WTs and a 111 kW SOFC.

Figure 4.2 shows the energy demand and generation of the first day of the control scenario with no constraint using the midpoint solution of 11 WTs and 9kW SOFC. The majority of the demand is begin met by the energy purchased from the grid with a small portion being met by the SOFC which remains at a constant output of 9kW after 06:00. In contrast, figure 4.3 displays the same day using the MG design parameters of the mid-point solution in the constrained control scenario, 1 PV, 25 WT and 11 kW SOFC.

The MG does not purchase any energy from the grid as per the constraint and the majority of the demand is met by the SOFC. There are periods of moderate wind generation and in these periods the SOFC generates less allowing the demand to be met by the wind. At 22:00 there is a spike in wind generation, however, because there is no BESS, this energy surplus is sold to the upstream grid. As there is no BESS or EVs present, no peak shaving occurs in these scenarios.

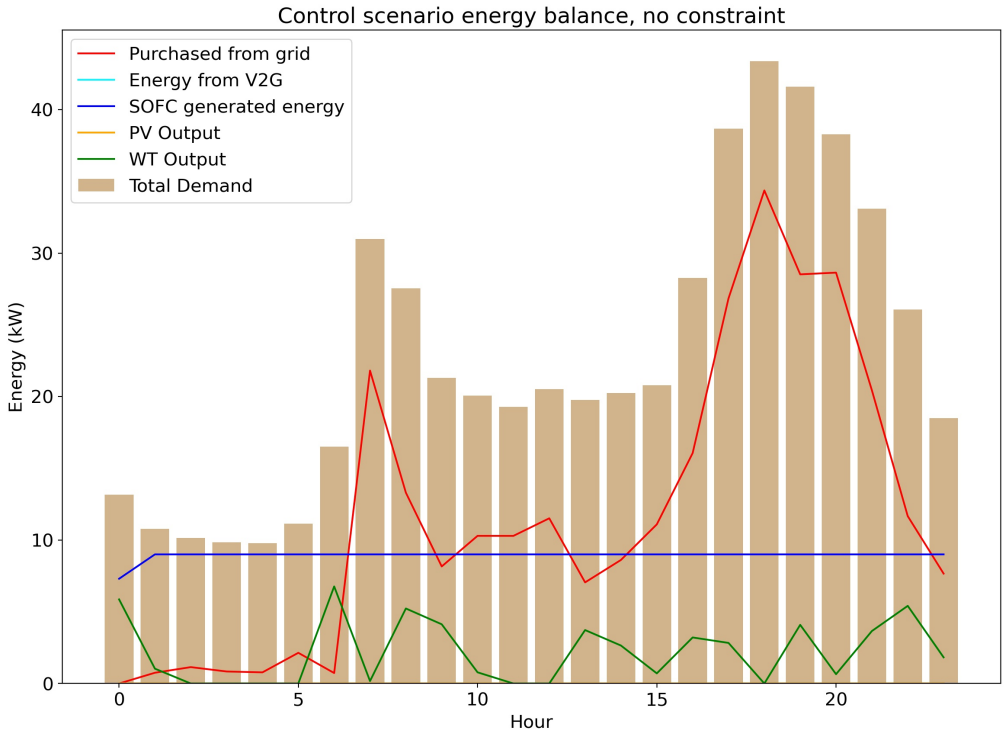

Figure 4.2: Control scenario day 1 energy balance

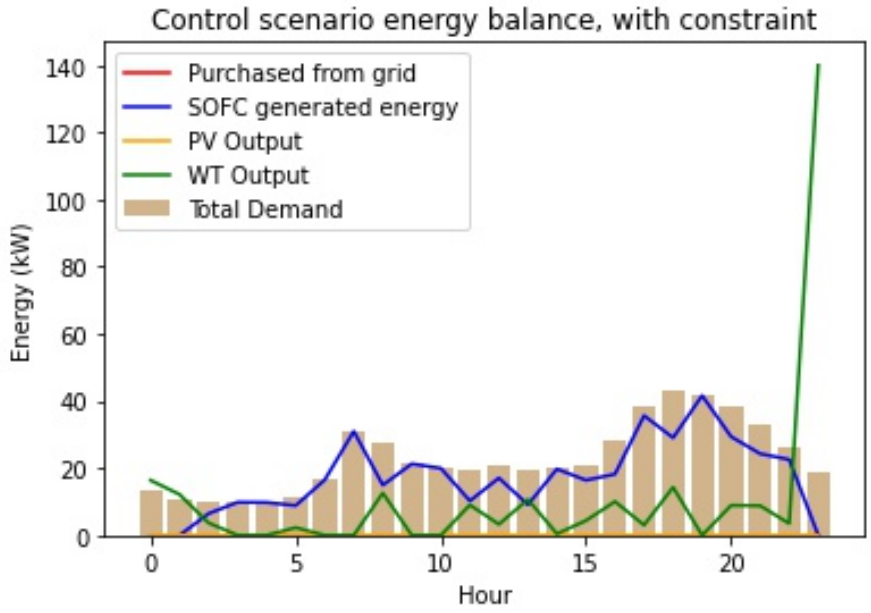

Figure 4.3: Control scenario day 1 energy balance with constraint

4.0.1.2 Scenario 1

As shown in blue in figure 4.4, scenario 1 with no constraint produced fewer non-dominated solutions than the control scenario and they are more scattered and not aligned to a near optimal front. The LCOE range is also lower with the cheapest solution being £68.39 and the most expensive being £255.62 compared to a high of £409 in the control scenario with no constraint. The range of LCA values is however higher, ranging from 1099.14 to 1295.13.

The cheapest solution in scenario 1 with no constraint had a LCOE of £68.39 and LCA of 1289.42 and design parameters of 1 PV, 2 WT and a 2 kW SOFC. The highest cost but lowest emissions solutions had an LCOE of

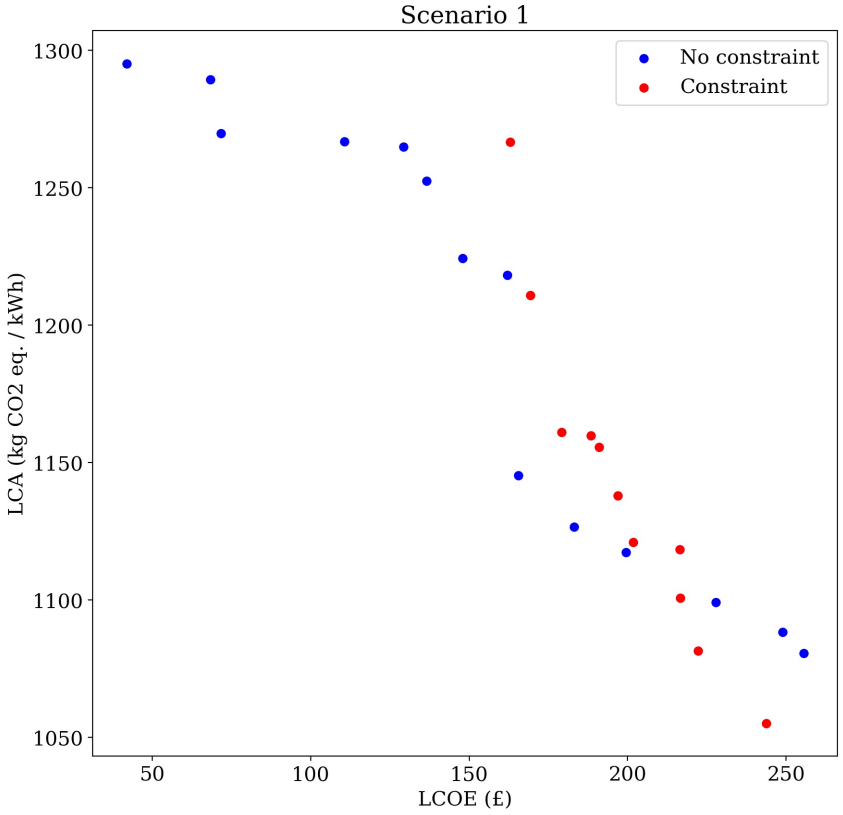

Figure 4.4: Scenario 1 results set

£255.62 and LCA of 1080.622 and design parameter of 17 PV, 21 WT and a 460kW SOFC. In the middle of the set, the solution has an LCOE of £147.89 and LCA of 12223.36 and design parameters of 6 PV, 24 WT and a 9 kW SOFC.

The results for constrained scenario 1, shown in red in figure 4.4, were on average more expensive, than the unconstrained solutions, with the minimum cost being £162.99. However, the most expensive constrained solution has a LCOE of £243.82 whereas the most expensive unconstrained solutions has

an LCOE of £255.62. The LCA values for the constrained and unconstrained solutions fall within the same range.

Figure 4.2 displays the energy demand and generation for the first day of scenario 1 using the mid-point solution design parameters with no constraints. For the peaks in demand during the day, namely 07:00 and between 17:00 and 20:00, the majority of the demand is being met by energy from V2G services. This contributes to making the MG almost £170 cheaper than the constrained control scenario mid-point and over £50 than the unconstrained control scenario mid-point.

It is also noted that the overall demand during the day is higher than in the control scenario where there was no EVs. This is because while there are EVs providing V2G services, there are also some charging at the same time, increasing the demand on the grid. In the control scenario, the average hourly energy demand was 22.90 kW, whereas in scenario 1, this increases to 38.91, which is a 70% increase.

In scenario 1, the total consumption over the simulation period was 10041 kWh and the energy provided to the grid through V2G was 4154 kWh. Meaning over 40% of demand was able to be met using V2G.

4.0.1.3 Scenario 2

The solution set produced in scenario 2 with no constraint is much sparser, as shown in blue in figure 4.6. There are only 4 non-dominated solutions and they fit closely into 2 groups. The cheapest solution but with the most emissions has an LCOE of £26.15 and LCA and 1307.08 with design parameters

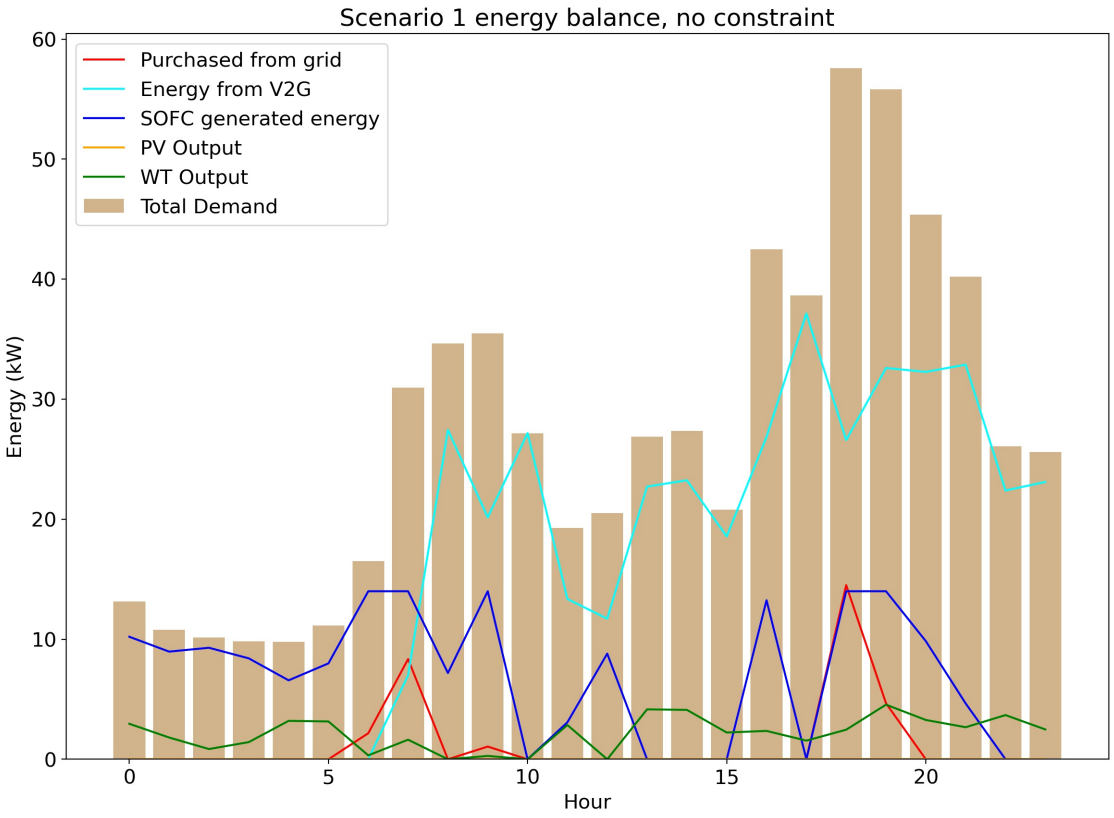

Figure 4.5: Scenario 1 day 1 energy balance with no constraint

of only 3 WTs. By comparison the solution in it's local cluster has an LCOE of £27.10 and LCA of 1236 by the only design difference is 5 PVs.

The difference between the higher cost and lower emissions solutions is more stark. The highest cost has design parameters of 8 PVs, 15 WTs and a 309 kW SOFC, however, its cluster neighbour is almost £30 cheaper with only an LVA value 4 higher. The highest price solution has design parameters of 8 PVs, 15 WTs and a 309 kW SOFC whereas its neighbour has 1 PV, 24 WTs, a 37 kW and a 1 kW BESS.

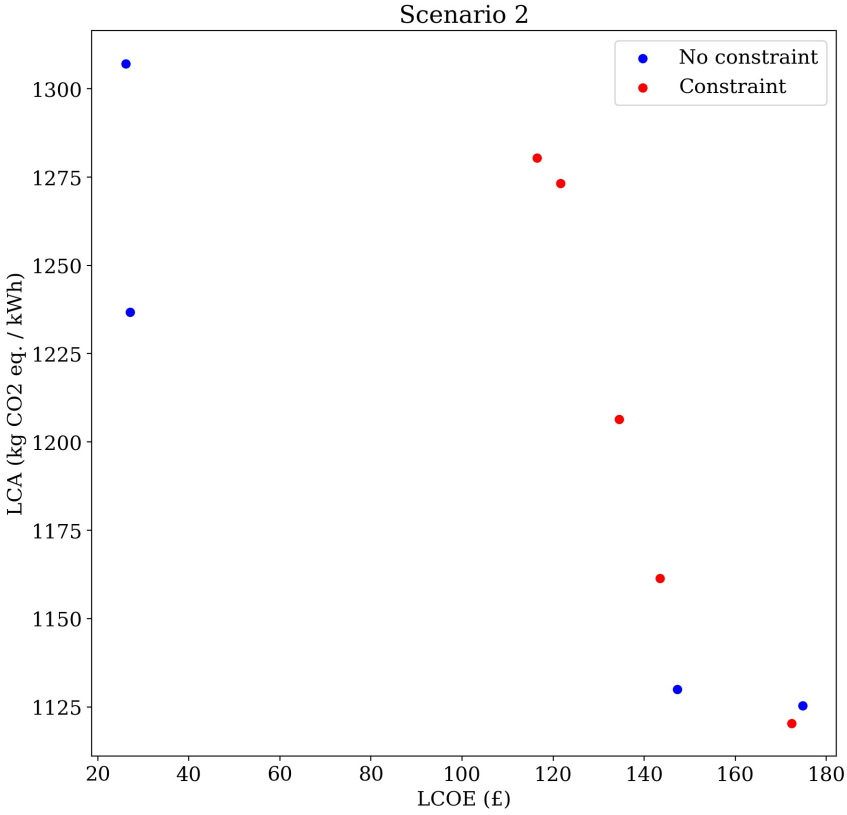

Figure 4.6: Scenario 2 result set

Scenario 2 with the constraint produces a slightly more diverse set of results, however they have very similar LCOE and LCA values to the unconstrained solutions, albeit the LCA is lower on average. All but one of the constrained solutions had a SOFC capacity of over 400 kW, more than 100 kW than the most expensive solution in the unconstrained scenario. This is because the SOFC is accommodating the demand of the MG rather than purchasing from the grid. The highest price solution with least emissions has a LCOE of £172.39 and LCA of 1120 has design parameters of 20 PVs, 3 WTs, a 411 kW SOFC and a 1 kW BESS. The cheapest solution with the

highest emissions has an LCOE of £116.43 and LCA of 128.39 and design parameters of 3 PVs, 47 WTs and a 498 kW SOFC.

In this scenario, it is clear that a high capacity SOFC is needed to ensure the autonomy of the grid. Accompanying that with a high number of PVs is an expensive solution but produces less emission, whereas using a high number of WTs instead is much cheaper but produces more emissions. This is reinforced by the solution at the mid-point that has design variables of 22 PVs, 32 WTs and a 219 kW SOFC. A balance in the number of PVs and WTs provides a balance in LCOE and LCA.

Using the design parameters from that mid-point in the 12 month simulation produces and energy balance shown in figure 4.7. As in scenario 2, the energy from V2G is providing the majority of the energy during the hours of highest demand. Before 06:00 when V2G can commence, the energy demand is met by a combination of WTs and the SOFC. When wind production drops, the SOFC steps in to fill the deficit. During the hours of highest demand between 18:00 and 21:00 the demand is predominantly met by the V2G energy without requiring any input from the SOFC.

While the increasing number of EVs is helping to meet demand, the consequence can be seen on day 2 of the simulation. A shown in figure **??**, there is a large energy demand in the early hours of the morning between 00:00 and 06:00 as all the vehicles are charging for the day in the time of cheapest electricity cost. The presence of 30 EVs in the MG almost doubles the average hourly demand from 22.90 kW in the control scenario to 42.19 in scenario 3.

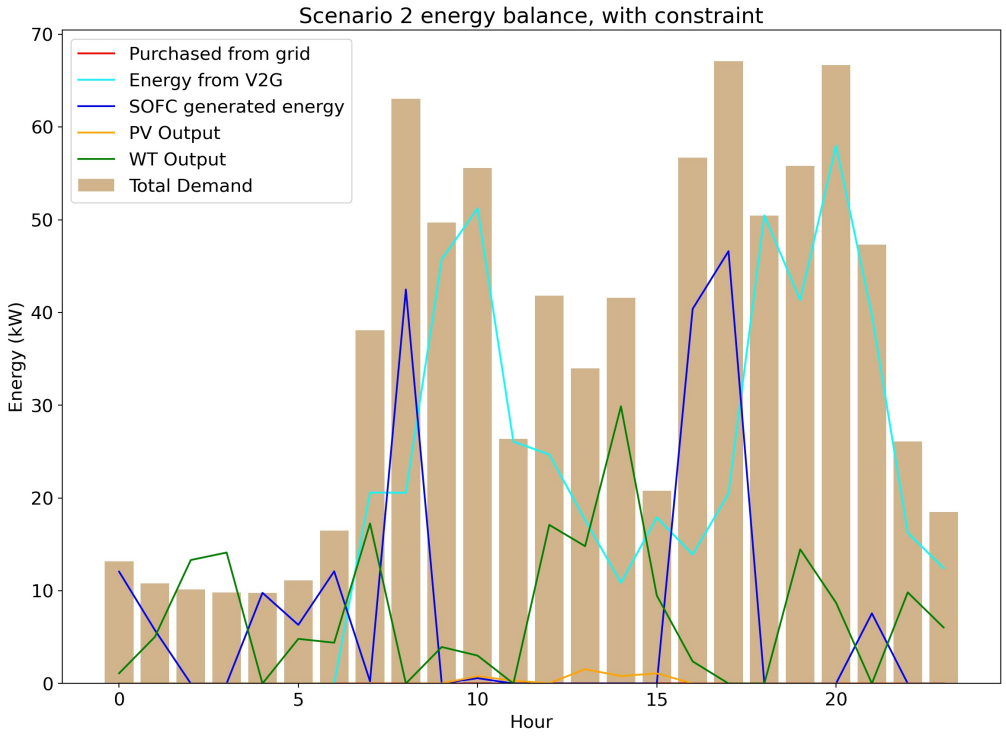

Figure 4.7: Scenario 2 energy balance on day 1

Figure 4.8 and 4.9 compares the SOC profiles of 3 EVs from scenario 2 over the course of day 1 and day 7 of simulation respectively.

In scenario 2, the total consumption over the simulation period was 11164 kWh and the energy provided to the grid through V2G was 6981 kWh. Meaning over 60% of demand was able to be met using V2G.

4.0.1.4 Scenario 3

In scenario 3, there is a reduction in the range of LCOE from scenario 2. In scenario 2 the LCOE ranges from £26.15 to £174 while in scenario 3 it

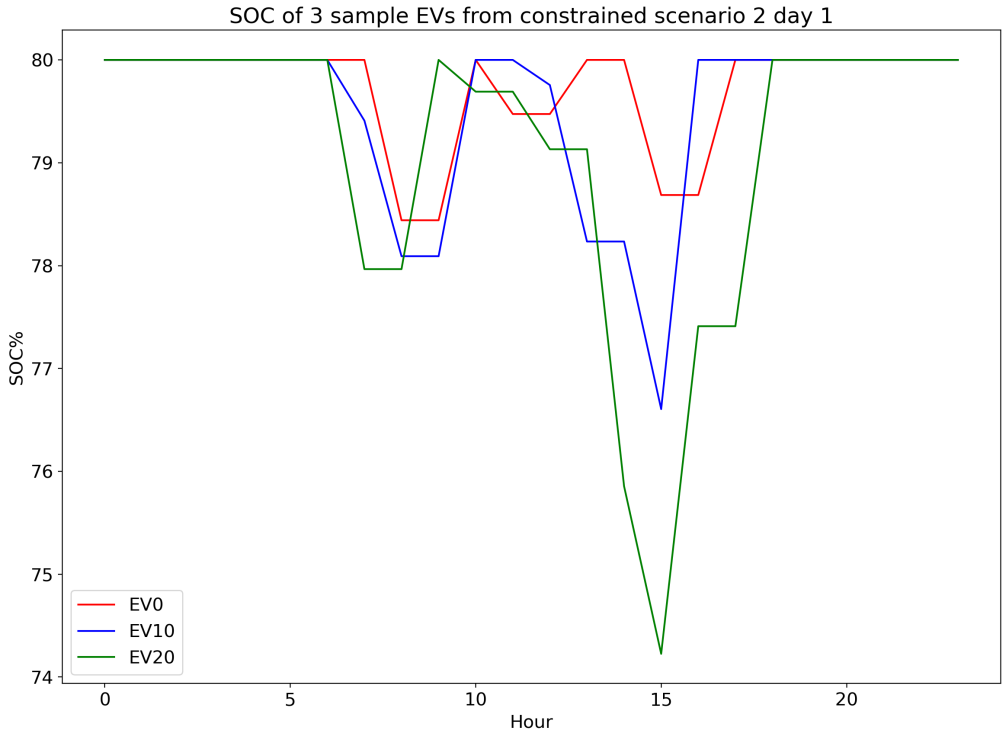

Figure 4.8: SOC of 3 sample EVs from constrained scenario 2 day 1

ranges from £22.08 to £169.21. In scenario 1 the range of LCOE values was £41.91 to £255.61, meaning there has been a 33.8% decrease in the upper limit of MG solution costs with an increase of 35 EVs and a of 58% decrease compared to the upper limit of the control scenario with no EVs. Therefore, despite the presence of EVs increasing the average hourly load of the MG, the costs of the MG decrease as their presence increases.

On the contrary, the increasing presence of EVs increases the emissions of the MG solutions in unconstrained scenarios. In the control scenario, the LCA values ranged from around 750 to just over 1150, whereas in scenario 3, the range is between 1169 and 1464. This is reduced in the constrained

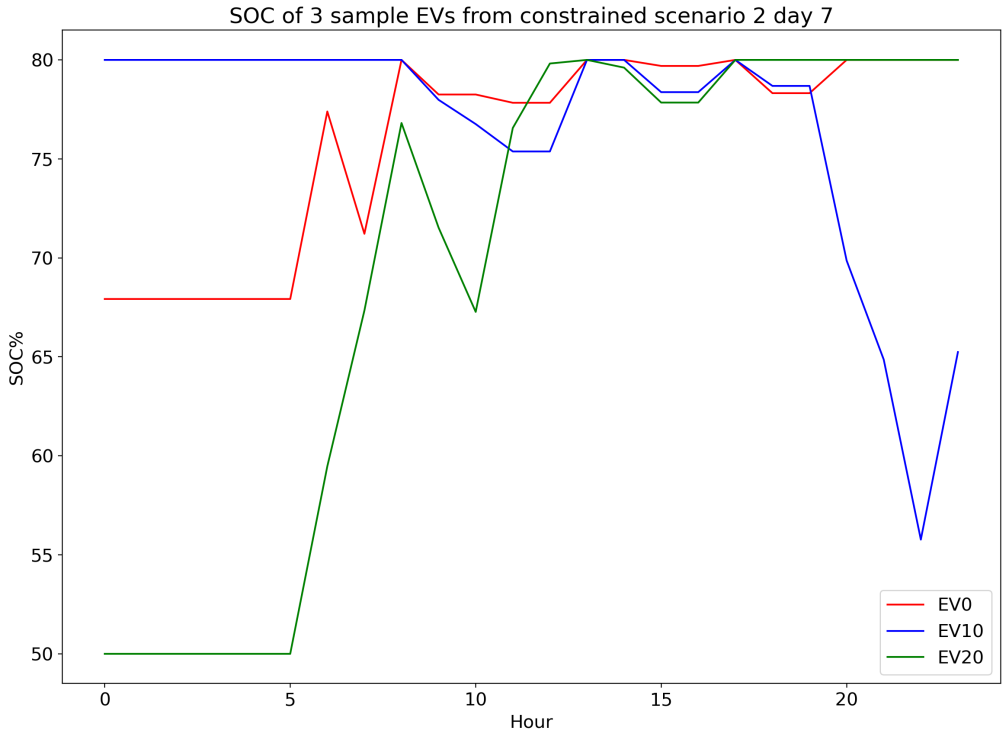

Figure 4.9: SOC of 3 sample EVs from constrained scenario 2 day 7

scenario to between 1180.29 and 1251.63. This indicates that while the increasing presence of EVs increases the demand for energy and therefore the emissions, solutions that rely on renewable energy over energy from the grid have lower LCA values.

The design parameters for the highest price, lowest emissions MG in scenario 3 are 61 PV, 8 WT and 156 kW SOFC. The design parameters for the lowest price, highest emissions MG in scenario 3 are 1 PV, and 1 WT. A solution in the middle of the set with a LCOE of 74.25 and LCA value of 1244.29 has design parameters of 8 PV, 1 WT, a 4 kW SOFC and a 1 kW BESS.

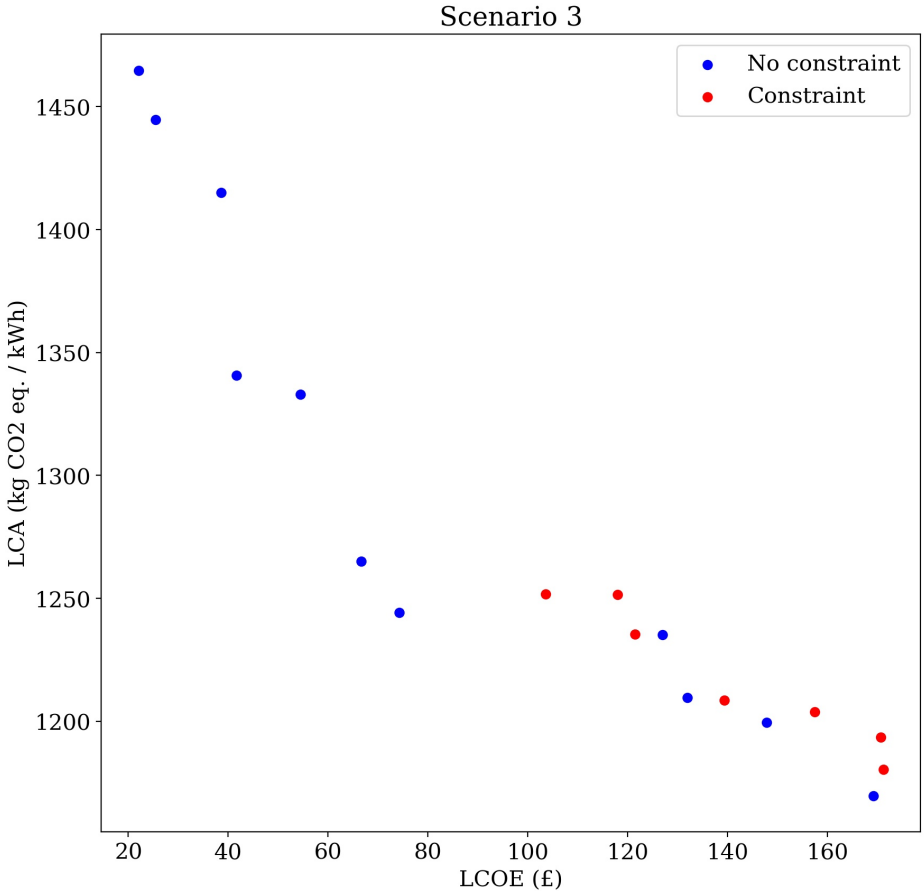

Figure 4.10: Scenario 2 result set

In the constrained scenario 3, the highest price, lowest emissions solutions had an LCOE of £171.18 and LCA value of 1180.29 and design parameters of 24 PV, 32 WT, a 452 kW SOFC and 2 kWh BESS. The design parameters for the lowest price, highest emissions MG are 10 PV, and 20 WT and a 401 kW SOFC. A mid-point solution with LCOE of £139.33 and LCA value of 1208.54 has design parameters of 20 PV, 21 WT, 308 kW SOFC and 1 kW BESS.

In scenario 3, the total consumption over the simulation period was 12705 kWh and the energy provided to the grid through V2G was 7854 kWh. Meaning over 60% of demand was able to be met using V2G.

These results demonstrate that the optimisation algorithm was able to find a range of appropriate MG designs under different levels of EV presence. Solutions that still relied on some energy from the grid had higher LCA values but were relatively cheap. Solutions that incorporated a large amount of one type of DER had low LCA values but were relatively expensive. Solutions that combined a mixture of DERs in proportional amouts found a balance between cost and emissions while also being able to maintain autonomy from the grid. The results also show that the presence of EVs within the grid played a large role in maintaining grid autonomy and reducing the cost of the MG. While EVs increased the overall energy demand of the grid, this increase in demand was balanced out by their ability to give back to the grid, showing them to be a useful flexible energy resource.

4.0.2 Impact on Objectives

The results support objective 1 as the optimisation algorithm found optimal MG parameters that found a balance between cost and environmental impact. While an increasing level of EVs helped to reduce the cost of the MG, it also increased the energy demand and in all scenarios the LCA values of the grid increased as the number of EVs increased. This means that the optimisation algorithm and V2G strategy alone were not sufficient to reduce the environmental impact of the gird and so objective 2 was not met. Despite

this, the results show very clearly that the MG was able to achieve autonomy from the grid due to the presence of EVs, and it was possible with even a small number of EVs such as in scenario 1. This means that objective 3 was successfully met.

Due to time limitations the secondary objectives were not met, however they are both important considerations for future research.

4.0.3 Limitations

While the results of this study are promising and 2 out of the 3 primary objectives were met, there are a couple of limitations that need to be considered. The simulation only considers supply and demand of energy and does not account for electrical network limitations such as voltage limits at electrical buses and current limits along electrical lines. It also assumes that the EV owners who live in the MG also work within the MG or the power from V2G is fed back to the MG while they are at work, however, depending on the size of the MG, it is unlikely the EVs will be connected to the same grid while at work and so the number of EVs able to provide power to the MG would be unknown. In addition, the current conditions for charging are fairly rigid. Despite incorporating the probability based V2G where participants have an 80% probability of choosing V2G when plugging in their car, more work needs to be done to account for uncertainty in EV driver charging behaviour. Finally, the BESS did not perform as expected.

Chapter 5

Conclusion

The aim of this study was to optimise the design of a residential MG using multi-objective optimisation while considering the presence of EVs and their role in the network. The results show that EVs have a substantial impact on the energy profile of a network. However, by integrating them into the design process, they can be leveraged as DERs to increase the autonomy and decrease the cost of the network. This has been shown in this paper through the use of the multi-objective optimisation algorithm NSGA-II, where candidate solutions are evaluated using a MAS based simulation. In simulations where the presence of EVs was above 50%, more than 60

Currently V2G capabilities are confined to the literature and a handful of small case study networks. With the number of EVs on the road set to increase exponentially in the coming years, it is imperative that their impacts be considered in network planning activities and the benefits of their active participation in power networks be incorporated in future planning.

Bibliography

Alanne, K. & Saari, A. (2006), 'Distributed energy generation and sustainable development', *Renewable & sustainable energy reviews* **10**(6), 539–558.

Anestis, A. & Georgios, V. (2019), 'Economic benefits of smart microgrids with penetration of der and mchp units for non-interconnected islands', *Renewable energy* **142**, 478–486.

Aquila, G., Rocha, L. C. S., Rotela Junior, P., Pamplona, E. d. O., Queiroz, A. R. d. & Paiva, A. P. d. (2016), 'Wind power generation: An impact analysis of incentive strategies for cleaner energy provision in brazil', *Journal of cleaner production* **137**, 1100–1108.

Atwa, Y., El-Saadany, E., Salama, M. & Seethapathy, R. (2010), 'Optimal renewable resources mix for distribution system energy loss minimization', *IEEE transactions on power systems* **25**(1), 360–370.

Ayadi, O., Shadid, R., Bani-Abdullah, A., Alrbai, M., Abu-Mualla, M. & Balah, N. (2022), 'Experimental comparison between monocrystalline, polycrystalline, and thin-film solar systems under sunny climatic conditions', *Energy reports* **8**, 218–230.

Basak, P., Chowdhury, S., Halder nee Dey, S. & Chowdhury, S. (2012), 'A literature review on integration of distributed energy resources in the perspective of control, protection and stability of microgrid', *Renewable sustainable energy reviews* **16**(8), 5545–5556.

BEIS (2022), 'Gas and electricity prices in the non-domestic sector', https://www.gov.uk/government/statistical-data-sets/gas-and-electricity-prices-in-the-non-domestic-sector. Accessed: 13 July 2022.

Boeing, G. (2017), 'Osmnx: New methods for acquiring, constructing, analyzing, and visualizing complex street networks', *Computers, environment and urban systems* **65**, 126–139.

Brouwer, A. S., Kuramochi, T., van den Broek, M. & Faaij, A. (2013), 'Fulfilling the electricity demand of electric vehicles in the long term future: An evaluation of centralized and decentralized power supply systems', *Applied energy* **107**(July 2013), 33–51.

Chaouachi, A., Kamel, R. M., Andoulsi, R. & Nagasaka, K. (2013), 'Multiobjective intelligent energy management for a microgrid', *IEEE transactions on industrial electronics (1982)* **60**(4), 1688–1699.

Chen, S. X., Gooi, H. B. & Wang, M. Q. (2012), 'Sizing of energy storage for microgrids', *IEEE transactions on smart grid* **3**(1), 142–151.

Cheng, T., Jiang, J., Wu, X., Li, X., Xu, M., Deng, Z. & Li, J. (2019), 'Application oriented multiple-objective optimization, analysis and comparison of solid oxide fuel cell systems with different configurations', *Applied energy* **235**, 914–929.

Choi, W., Kim, J., Kim, Y. & Song, H. H. (2019), 'Solid oxide fuel cell operation in a solid oxide fuel cell–internal combustion engine hybrid system and the design point performance of the hybrid system', *Applied energy* **254**, 113681.

Chowdhury, J. I., Balta-Ozkan, N., Goglio, P., Hu, Y., Varga, L. & McCabe, L. (2020), 'Techno-environmental analysis of battery storage for grid level energy services', *Renewable & sustainable energy reviews* **131**, 110018.

Dallinger, D. & Wietschel, M. (2012), 'Grid integration of intermittent renewable energy sources using price-responsive plug-in electric vehicles', *Renewable sustainable energy reviews* **16**(5), 3370–3382.

Das, A. & Balakrishnan, V. (2012), 'Sustainable energy future via grid interactive operation of spv system at isolated remote island', *Renewable sustainable energy reviews* **16**(7), 5430–5442.

Deb, K., Pratap, A., Agarwal, S. & Meyarivan, T. (2002), 'A fast and elitist multiobjective genetic algorithm: Nsga-ii', *IEEE transactions on evolutionary computation* **6**(2), 182–197.

Deng, N., Zhang, X.-P., Wang, P., Gu, X. & Wu, M. (2013), A converter-based general interface for ac microgrid integrating to the grid, *in* 'IEEE PES ISGT Europe 2013', IEEE, pp. 1–5.

DfT (2020), National travel survey: 2019, Technical report, Department for Transport, United Kingdom.

DfT (2022), Vehicle licensing statistics: January to march 2022, Technical report, Department for Transport, United Kingdom.

Dougier, N., Garambois, P., Gomand, J. & Roucoules, L. (2021), 'Multi-objective non-weighted optimization to explore new efficient design of electrical microgrids', *Applied energy* **304**, 117758.

ElectricVehicleDataBase (2022), 'Tesla model 3 long range dual motor', https://ev-database.uk/car/1321/Tesla-Model-3-Long-Range-Dual-Motor#similar. Online; Accessed: 1 June 2022.

Elmer, T., Worall, M., Wu, S. & Riffat, S. B. (2015), 'Emission and economic performance assessment of a solid oxide fuel cell micro-combined heat and power system in a domestic building', *Applied thermal engineering* **90**, 1082–1089.

EWT (2022), 'Directwind 52', https://ewtdirectwind.com/products/dw52/. Online; Accessed: 2 August 2022.

Faraji, J., Hashemi-Dezaki, H. & Ketabi, A. (2020), 'Optimal probabilistic scenario-based operation and scheduling of prosumer microgrids considering uncertainties of renewable energy sources', *Energy science & engineering* **8**(11), 3942–3960.

Fardadi, M., McLarty, D. F. & Jabbari, F. (2016), 'Investigation of thermal control for different sofc flow geometries', *Applied energy* **178**, 43–55.

Fathima, A. H. & Palanisamy, K. (2015), 'Optimization in microgrids with hybrid energy systems – a review', *Renewable & sustainable energy reviews* **45**, 431–446.

Gamarra, C. & Guerrero, J. M. (2015), 'Computational optimization techniques applied to microgrids planning: A review', *Renewable sustainable energy reviews* **48**, 413–424.

García-Villalobos, J., Zamora, I., San Martín, J., Asensio, F. & Aperribay, V. (2014), 'Plug-in electric vehicles in electric distribution networks: A review of smart charging approaches', *Renewable sustainable energy reviews* **38**, 717–731.

Gillies, S. et al. (2007–), 'Shapely: manipulation and analysis of geometric objects'.
URL: *https://github.com/Toblerity/Shapely*

Hadley, S. W. & Tsvetkova, A. A. (2009), 'Potential impacts of plug-in hybrid electric vehicles on regional power generation', *The Electricity journal* **22**(10), 56–68.

Hagberg, A. A., Schult, D. A. & Swart, P. J. (2008), Exploring network structure, dynamics, and function using networkx, *in* G. Varoquaux, T. Vaught & J. Millman, eds, 'Proceedings of the 7th Python in Science Conference', Pasadena, CA USA, pp. 11 – 15.

Hemmati, R. (2017), 'Technical and economic analysis of home energy management system incorporating small-scale wind turbine and battery energy storage system', *Journal of cleaner production* **159**, 106–118.

Hetzer, J., Yu, D. & Bhattarai, K. (2008), 'An economic dispatch model incorporating wind power', *IEEE transactions on energy conversion* **23**(2), 603–611.

Hu, B., Wang, S., Zhang, X., Wang, T., Qu, F., Zheng, W. & Zhou, B. (2019), 'Power grid peak shaving strategies based on electric vehicles and thermal storage electric boilers', *IOP conference series. Earth and environmental science* **227**(3), 32026.

IEA (2019), Global ev outlook 2019, Technical report, IEA, Paris.

IEA (2020), Projected costs of generating electricity 2020, Technical report, IEA, Paris.

IEA (2021), 'Electric vehicles', https://www.iea.org/reports/electric-vehicles. Online; Accessed 20 March 2022.

IEA (2022), 'Electricity market report - january 2022'. Online; Accessed: 20 April 2022.
URL: *https://www.iea.org/reports/electricity-market-report-january-2022*

Jiang, J., Zhou, R., Xu, H., Wang, H., Wu, P., Wang, Z. & Li, J. (2022), 'Optimal sizing, operation strategy and case study of a grid-connected solid oxide fuel cell microgrid', *Applied energy* **307**, 118214.

Jordahl, K., den Bossche, J. V., Fleischmann, M., Wasserman, J., McBride, J., Gerard, J., Tratner, J., Perry, M., Badaracco, A. G., Farmer, C., Hjelle, G. A., Snow, A. D., Cochran, M., Gillies, S., Culbertson, L., Bartos, M., Eubank, N., maxalbert, Bilogur, A., Rey, S., Ren, C., Arribas-Bel, D., Wasser, L., Wolf, L. J., Journois, M., Wilson, J., Greenhall, A., Holdgraf, C., Filipe & Leblanc, F. (2020), 'geopandas/geopandas: v0.8.1'.
URL: *https://doi.org/10.5281/zenodo.3946761*

Katiraei, F. & Iravani, M. (2006), 'Power management strategies for a microgrid with multiple distributed generation units', **21**(4), 1821–1831.

Katsigiannis, Y., Georgilakis, P. & Karapidakis, E. (2010), 'Multi-objective genetic algorithm solution to the optimum economic and environmental performance problem of small autonomous hybrid power systems with renewable', *Renewable Power Generation, IET* **4**, 404 – 419.

Kazil, J., Masad, D. & Crooks, A. (2020), Utilizing python for agent-based modeling: The mesa framework, *in* R. Thomson, H. Bisgin, C. Dancy, A. Hyder & M. Hussain, eds, 'Social, Cultural, and Behavioral Modeling', Springer International Publishing, Cham, pp. 308–317.

Kefayat, M., Lashkar Ara, A. & Nabavi Niaki, S. (2015), 'A hybrid of ant colony optimization and artificial bee colony algorithm for probabilistic optimal placement and sizing of distributed energy resources', *Energy conversion and management* **92**, 149–161.

Kempton, W. & Letendre, S. E. (1997), 'Electric vehicles as a new power source for electric utilities', *Transportation research. Part D, Transport and environment* **2**(3), 157–175.

Langnickel, H., Rautanen, M., Gandiglio, M., Santarelli, M., Hakala, T., Acri, M. & Kiviaho, J. (2020), 'Efficiency analysis of 50 kwe sofc systems fueled with biogas from waste water', *Journal of Power Sources Advances* **2**, 100009.

Liu, Z., Chen, Y., Zhuo, R. & Jia, H. (2018), 'Energy storage capacity op-

timization for autonomy microgrid considering chp and ev scheduling', *Applied energy* **210**, 1113–1125.

Loh, P. C., Li, D., Chai, Y. K. & Blaabjerg, F. (2013), 'Hybrid ac-dc microgrids with energy storages and progressive energy flow tuning', *IEEE transactions on power electronics* **28**(4), 1533–1543.

Lopes, J. A. P., Madureira, A. G. & Moreira, C. C. L. M. (2013), 'A view of microgrids', *Wiley interdisciplinary reviews. Energy and environment* **2**(1), 86–103.

Lotfi, H. & Khodaei, A. (2017), 'Hybrid ac/dc microgrid planning', *Energy (Oxford)* **118**, 37–46.

Marmaras, C., Xydas, E. & Cipcigan, L. (2017), 'Simulation of electric vehicle driver behaviour in road transport and electric power networks', *Transportation research. Part C, Emerging technologies* **80**, 239–256.

Mehigan, L., Deane, J., Gallachóir, B. & Bertsch, V. (2018), 'A review of the role of distributed generation (dg) in future electricity systems', *Energy (Oxford)* **163**, 822–836.

Meyer, J. (2022), '5 best solar panels in the uk [2022 reviews]', https://www.ecowatch.com/best-solar-panels-uk.html. Online; Accessed: 10 June 2022.

Moghateli, F., Taher, S. A., Karimi, A. & Shahidehpour, M. (2020), 'Multi-objective design method for construction of multi-microgrid systems in active distribution networks', *IET Smart Grid* **3**(3), 331–341.

Morvaj, B., Evins, R. & Carmeliet, J. (2016), 'Optimization framework for distributed energy systems with integrated electrical grid constraints', **171**, 296–313.

Mwasilu, F., Justo, J. J., Kim, E.-K., Do, T. D. & Jung, J.-W. (2014), 'Electric vehicles and smart grid interaction: A review on vehicle to grid and renewable energy sources integration', *Renewable sustainable energy reviews* **34**, 501–516.

Napoli, R., Gandiglio, M., Lanzini, A. & Santarelli, M. (2015), 'Techno-economic analysis of pemfc and sofc micro-chp fuel cell systems for the residential sector', *Energy and buildings* **103**, 131–146.

Nikmehr, N. & Ravadanegh, S. N. (2015), 'Optimal power dispatch of multi-microgrids at future smart distribution grids', *IEEE transactions on smart grid* **6**(4), 1648–1657.

Ogunjuyigbe, A., Ayodele, T. & Akinola, O. (2016), 'Optimal allocation and sizing of pv/wind/split-diesel/battery hybrid energy system for minimizing life cycle cost, carbon emission and dump energy of remote residential building', *Applied energy* **171**, 153–171.

Omu, A., Choudhary, R. & Boies, A. (2013), 'Distributed energy resource system optimisation using mixed integer linear programming', *Energy policy* **61**, 249–266.

O'Neill, D., Yildiz, B. & Bilbao, J. I. (2022), 'An assessment of electric vehicles and vehicle to grid operations for residential microgrids', *Energy reports* **8**, 4104–4116.

Paoli, L. & Gül, T. (2022), 'Electric cars fend off supply challenges to more than double global sales'. Online; Accessed: 28 February 2022.
URL: *https://www.iea.org/commentaries/electric-cars-fend-off-supply-challenges-to-more-than-double-global-sales*

Patrao, I., Figueres, E., Garcerá, G. & González-Medina, R. (2015), 'Microgrid architectures for low voltage distributed generation', *Renewable & sustainable energy reviews* **43**, 415–424.

Pfeifroth, U., Kothe, S., Müller, R., Trentmann, J., Hollmann, R., F. P. & Werscheck, M. (2017), 'Surface radiation data set - heliosat (sarah) - edition 2'.

Planas, E., Gil-de Muro, A., Andreu, J., Kortabarria, I. & Martínez de Alegría, I. (2013), 'General aspects, hierarchical controls and droop methods in microgrids: A review', *Renewable sustainable energy reviews* **17**(1), 147–159.

Pullinger, M., Kilgour, J., Goddard, N., Berliner, N., Webb, L., Dzikovska, M., Lovell, H., Mann, J., Sutton, C., Webb, J. & Zhong, M. (2021), 'The ideal household energy dataset, electricity, gas, contextual sensor data and survey data for 255 uk homes', *Scientific data* **8**(1), 146–146.

Quiggin, D., Cornell, S., Tierney, M. & Buswell, R. (2012), 'A simulation and optimisation study: Towards a decentralised microgrid, using real world fluctuation data', *Energy (Oxford)* **41**(1), 549–559.

Rabiee, A., Sadeghi, M., Aghaeic, J. & Heidari, A. (2016), 'Optimal operation of microgrids through simultaneous scheduling of electrical vehicles and

responsive loads considering wind and pv units uncertainties', *Renewable & sustainable energy reviews* **57**, 721–739.

Rakhshani, E., Mehrjerdi, H. & Iqbal, A. (2020), 'Hybrid wind-diesel-battery system planning considering multiple different wind turbine technologies installation', *Journal of cleaner production* **247**, 119654.

Ramachandran, B., Srivastava, S. K. & Cartes, D. A. (2013), 'Intelligent power management in micro grids with ev penetration', *Expert systems with applications* **40**(16), 6631–6640.

Ren, H. & Gao, W. (2010), 'A milp model for integrated plan and evaluation of distributed energy systems', *Applied energy* **87**(3), 1001–1014.

Rillo, E., Gandiglio, M., Lanzini, A., Bobba, S., Santarelli, M. & Blengini, G. (2017), 'Life cycle assessment (lca) of biogas-fed solid oxide fuel cell (sofc) plant', *Energy (Oxford)* **126**, 585–602.

Roslan, M., Hannan, M., Ker, P. J. & Uddin, M. (2019), 'Microgrid control methods toward achieving sustainable energy management', *Applied energy* **240**, 583–607.

Saber, A. & Venayagamoorthy, G. (2011), 'Plug-in vehicles and renewable energy sources for cost and emission reductions', *IEEE transactions on industrial electronics (1982)* **58**(4), 1229–1238.

Sachs, J. & Sawodny, O. (2016), 'Multi-objective three stage design optimization for island microgrids', *Applied energy* **165**, 789–800.

Samadi Gazijahani, F. & Salehi, J. (2017), 'Stochastic multi-objective framework for optimal dynamic planning of interconnected microgrids', *IET renewable power generation* **11**(14), 1749–1759.

SDWindEnergy (2022), 'Sd6 6kw small wind turbine', https://sdwindenergy.com/small-wind-turbines/sd6-6kw-wind-turbine/. Online; Accessed: 2 August 2022.

SunPower (2022), 'Maxeon 3 dc, 390-400 w product datasheet', https://sunpower.maxeon.com/uk/solar-panel-products/maxeon-solar-panels. Online; Accessed: 10 June 2022.

Tan, K. M., Ramachandaramurthy, V. K. & Yong, J. Y. (2016), 'Integration of electric vehicles in smart grid: A review on vehicle to grid technologies and optimization techniques', *Renewable & sustainable energy reviews* **53**, 720–732.

Tushar, M. H. K., Assi, C., Maier, M. & Uddin, M. F. (2014), 'Smart microgrids: Optimal joint scheduling for electric vehicles and home appliances', *IEEE transactions on smart grid* **5**(1), 239–250.

UK, G. (2022), 'Low-emission vehicles eligible for a plug-in grant'. Online; Accessed: 20 April 2022.
URL: *https://www.gov.uk/plug-in-vehicle-grants*

Wang, Y., Sun, Y., Zhang, Y., Chen, X., Shen, H., Liu, Y., Zhang, X. & Zhang, Y. (2022), 'Optimal modeling and analysis of microgrid lithium iron phosphate battery energy storage system under different power supply states', *Journal of power sources* **521**, 230931.

Wang, Z., Chen, B., Wang, J., Kim, J. & Begovic, M. M. (2014), 'Robust optimization based optimal dg placement in microgrids', *IEEE transactions on smart grid* **5**(5), 2173–2182.

Wasilewski, J. (2018), 'Optimisation of multicarrier microgrid layout using selected metaheuristics', *International journal of electrical power energy systems* **99**, 246–260.

Zahedi, A. (2011), 'A review of drivers, benefits, and challenges in integrating renewable energy sources into electricity grid', *Renewable & sustainable energy reviews* **15**(9), 4775–4779.

Zia, M. F., Elbouchikhi, E. & Benbouzid, M. (2018), 'Microgrids energy management systems: A critical review on methods, solutions, and prospects', *Applied energy* **222**, 1033–1055.

Zidan, A., Gabbar, H. A. & Eldessouky, A. (2015), 'Optimal planning of combined heat and power systems within microgrids', *Energy (Oxford)* **93**, 235–244.